U. S. AIR FORCE

PROJECT RAND

RESEARCH MEMORANDUM

INFRARED TECHNIQUES APPLIED TO THE DETECTION AND INTERCEPTION OF INTERCONTINENTAL BALLISTIC MISSILES

William W. Kellogg
Sidney Passman

RM-1572

ASTIA Document Number AD 114176

October 21, 1955

This research is sponsored by the United States Air Force under cantract No. AF 49(638)-700 monitored by the Directorate of Development Planning, Deputy Chief of Staff, Research and Technology, Hq USAF.

This is a working paper. Because it may be expanded, modified, or withdrawn at any time, permission to quote or reproduce must be obtained from RAND. The views, conclusians, and recommendations expressed herein do not necessarily reflect the official views or policies of the United States Air Force.

DISTRIBUTION RESTRICTIONS

67 pps

The RAND Corporation
1700 MAIN ST., SANTA MONICA, CALIFORNIA

SUMMARY

The defensive application of infrared-optical techniques for the detection of an intercontinental ballistic missile (ICBM) during its takeoff, midcourse flight, and re-entry is considered quantitatively in terms of maximum detection ranges and times for tracking.

The re-entry phase is examined from the point of view of an infrared tracking head in an interceptor missile. The times between first acquisition by this tracker and the interception are presented in terms of interceptor altitude and ICBM re-entry angle for several types of re-entry bodies.

The takeoff phase is examined from the point of view of an early-warning system employing an airborne infrared search set at 40,000 ft altitude stationed outside of enemy territory. The detection ranges are presented as a function of missile altitude, and the effects of the horizon (modified by the presence of clouds below the search station) and the horizontal travel of the missile from the launching site are taken into account. It is shown that such a system can probably detect (and track) missiles up to burnout with launching-site-to-detection-station distances of the order of 1400 n mi.

The optical detection of an ICBM during its midcourse flight after burnout is apparently possible only under a rather limited set of conditions, i.e., at twilight, when the ICBM is in the sunlight but the detector is in the earth's shadow. In this application a photomultiplier detector system operating in the visible portion of the spectrum appears to be superior to an infrared system.

CONTENTS

SUMMARY..... ii

Section
I. INTRODUCTION..... 1

II. CALCULATION OF MAXIMUM DETECTION RANGES DURING RE-ENTRY OF AN ICBM..... 3
A. Basic Range Equation..... 3
B. ICBM Emission During Re-Entry..... 4
C. Minimum Detectable Flux and Spectral Response of the Detection System..... 10
D. Maximum Detection Ranges During Re-Entry..... 21
E. Discrimination against the Star Background..... 26
F. Meteors, a Natural Decoy..... 28

III. CALCULATION OF MAXIMUM DETECTION RANGES DURING TAKE-OFF OF AN ICBM..... 29
A. ICBM Emission During Take-off..... 30
B. Geometrical Limitations on Detection Ranges Due to Curvature of the Earth and the Trajectory of the Missile. 37
C. Limiting Sensitivity of an Infrared Search System..... 46
D. Maximum Detection Ranges During Take-off..... 49

IV. DETECTION OF AN ICBM DURING ITS MID-COURSE FLIGHT..... 53
A. ICBM Emission During Mid-Course Flight..... 53
B. Intensity of Reflected Sunlight Signal..... 54
C. Sensitivity of a Photoelectric Detection System..... 56
D. Detection Ranges..... 57

V. FIELDS FOR FURTHER RESEARCH..... 60
A. Re-Entry..... 60
B. Take-off..... 61

REFERENCES..... 63

I. INTRODUCTION

It appears to be a basic characteristic of an ICBM that aerodynamic heating causes it to get hot during takeoff and even hotter during re-entry into the atmosphere. Since hot metal is a good emitter of infrared radiation, it would be expected that the missile could be detected by infrared detectors during its flight through the atmosphere. The emission of infrared radiation by the rocket flame during the boost stage further increases this expectation, with the added possibility that there may be enough radiation to permit infrared detection during that part of the powered flight which occurs above the atmosphere. The purpose of this report is to pull together the various factors involved in determining how such a detector system would work, and to show some estimated detection ranges, based on a reasonable extrapolation of the current capabilities in infrared detection systems and photo-conductor cells.

Although it is indeed possible to make such estimates, it must be emphasized at the outset that there are too many variables in the problem to permit a precise answer. To name a few of the uncertainties:

- The description of an ICBM must be rather vague, since, so far as we know, none has ever been built. In this study four possible re-entry configurations have been selected from the many possibilities. The selection is intended to bracket the most likely types.
- The requirements on a detection system in terms of the amount of information it must provide, the angular accuracy, the time available, etc., will determine the minimum infrared signal with which it can work. Therefore, it is necessary to make some rather arbitrary assumptions about the way in which the system will be employed before

one can estimate such a parameter as the maximum detection range.

- During the takeoff of an ICBM the rocket flame must emit a great deal of infrared radiation. A fairly exhaustive survey has failed to lead to a satisfactory description of the emission of a rocket flame in a vacuum, as would be encountered during the later part of the boosted flight. This is being investigated further at RAND, but for the time being we must content ourselves with a rough estimate of this quantity.

Thus, the answers are still incomplete. Even so, some very significant results can be obtained. It appears that infrared detection systems operating in a favorable environment will have a good chance of detecting ICBM's during takeoff and re-entry at ranges long enough to be useful defensively. It should be borne in mind that the only apparent alternative to an infrared detection system -- namely, a radar detection system -- offers serious problems because of the small radar cross-section of the missiles and the requirements for high angular accuracy.

An important function will have been fulfilled if this study can stimulate further work in the field of ICBM detection by optical-infrared methods. A number of fruitful areas for research will be suggested in the course of the report, and are summarized at the end in Chapt. V.

II. CALCULATION OF MAXIMUM DETECTION RANGES DURING RE-ENTRY OF AN ICBM

Interest in active defense against the ICBM has centered around systems for intercepting the missile during the re-entry phase of its flight. Therefore, the problem of infrared detection during this phase will be considered first. The analysis given here will serve as the groundwork for analyzing the problems of detection during other phases of the flight.

A. BASIC RANGE EQUATION

It is possible to solve the equation expressing the limiting condition for infrared detection explicitly in terms of the maximum detection range:*

$$R_{max} = \sqrt{\frac{\epsilon J A_T}{\pi} \frac{\eta_w \eta_f \eta_s}{P_t}}$$

where: ϵ is the total emissivity of the source, assumed independent of wavelength (equals unity for a "black body")

J is the total black body emission of the source per unit area

A_T is the total projected area of the source or target

η_w is the fraction of flux emitted which is transmitted by the atmosphere

η_f is the fraction of flux reaching the detector which is transmitted to the cell, after the action of color filters in the system.

η_s is the fraction of flux reaching the cell which is detected by the cell

*For a derivation of the equation in this form, and a discussion of the various parameters involved, see Ref. (1). A good discussion of the specific problem of ballistic missile detection by infrared emission is also contained in Ref. (2).

P_t is the minimum effective flux from the target which will provide the seeker with reliable guidance information

For investigating detection ranges against ICBM's, this equation can be simplified by grouping together certain parameters:

$$R_{max} = \sqrt{\frac{E_T \eta_D}{\pi P_t}} \times \sqrt{\eta_\omega} \qquad (1)$$

where: E_T is the total black body emission of the source or target, which is equal to $\epsilon J A_T$.

η_D is the spectral efficiency of the detection system, which is equal to $\eta_s \eta_f$.

Note: It is assumed that $\eta_\omega = 1$ in the re-entry calculations below, where detection is made at very high altitude.

It will be noted that the factor E_T, the target emission, is a function of the configuration of the target, its temperature, and its emissivity, while all the other factors in the first radical are functions of the detection system. For this reason, it is convenient to investigate the target first, and then choose the characteristics of the detection system so that they will tend to maximize the range and at the same time fulfill the operational requirements for speed and accuracy. In each chapter this procedure is followed, since the emission characteristics of the target and the operational constraints on detection are quite different during the various phases of the flight.

B. ICBM EMISSION DURING RE-ENTRY

As an ICBM re-enters the earth's atmosphere (after spending twenty to

thirty minutes in what may be considered as interplanetary space) it suffers violent decelerations, and its skin temperature increases at a rate which is roughly proportional to the deceleration.[3] While the problem of designing a missile re-entry body and warhead which can withstand the unique heating rate encountered in high speed re-entry of the atmosphere is a formidable one, it appears that several approaches might be successful.[3][4] Since we cannot yet know which alternative the enemy will choose, it is necessary to treat enough cases to give some idea of the behavior of the family of possible configurations.

A description of four possible re-entry systems is given in Table 1. Assuming an initial re-entry velocity of 23,700 ft/sec, characteristic of a 5,500 mi ICBM fired on its minimum-energy trajectory (with a re-entry angle of about 22 degrees from the horizontal) the corresponding frontal skin temperatures for the four cases are shown in Fig. 1 as a function of altitude.* The corresponding total emitted radiation from the target in the forward aspect is given in Fig. 2. A total emissivity, ϵ, of 0.8 was used for the first three cases, since this is roughly representative of a variety of oxidized metallic surfaces and of graphite. The fourth case, where the surface is oxidized copper, has an emissivity of about 0.5. A polished metal surface would have a lower emissivity, but it is believed that the surface would become oxidized and perhaps roughened during its passage through the atmosphere.

It is clear that the various re-entry characteristics differ markedly and therefore pose very different detection and interception problems during the re-entry phase. It should be borne in mind that the infrared emission

*Calculations of skin temperatures were made by C. Gazley and M. C. Horn, RAND Missiles Division, for Cases 1, 2 and 3; by Convair for Case 4 (Ref. 5).

TABLE I

CHARACTERISTICS OF FOUR POSSIBLE RE-ENTRY SYSTEMS

CASE	DESCRIPTION OF RE-ENTRY CONFIGURATION	$\frac{C_D A}{W \sin \theta}$ *	FRONTAL AREA (ft^2)
(1) High-speed re-entry body	10° half-angle cone .02-in hastalloy skin W/A $\cong$ 250 lbs/ft^2 (Temps. calculated 1 ft from apex of nose.)	10^{-3}	7.1
(2) High-speed re-entry body	30° half-angle cone 1-in graphite skin W/A $\cong$ 150 lbs/ft^2 (Temps. calculated 2.5 ft from apex of nose.)	1-2 x 10^{-2}	7.1
(3) Low-speed re-entry body: 106-in drag skirt. Separation of skirt when velocity is 5000 ft/sec at an alt. of 98,000 ft.	Before separation: 60° half-angle cone Thick graphite or thin metal skin -- a compromise between cases (1) and (2). W/A $\cong$ 37.5 lbs/ft^2	0.1	61.5
	After separation: 30° half-angle cone Same skin W/A $\cong$ 150 lbs/ft^2	1-2 x 10^{-2}	7.1
(4) High-speed re-entry body	Rounded cone with 40° effective half-angle 1 1/4-in copper skin W/A $\cong$ 350 lbs/ft^2	10^{-2}	10.5

*Parameter used by Gazley in computing the rate of heat input[3]; W is the weight of the re-entry body (lbs), A is the frontal area (ft^2), C_D is the drag coefficient, and θ is the re-entry angle, measured from the horizon.

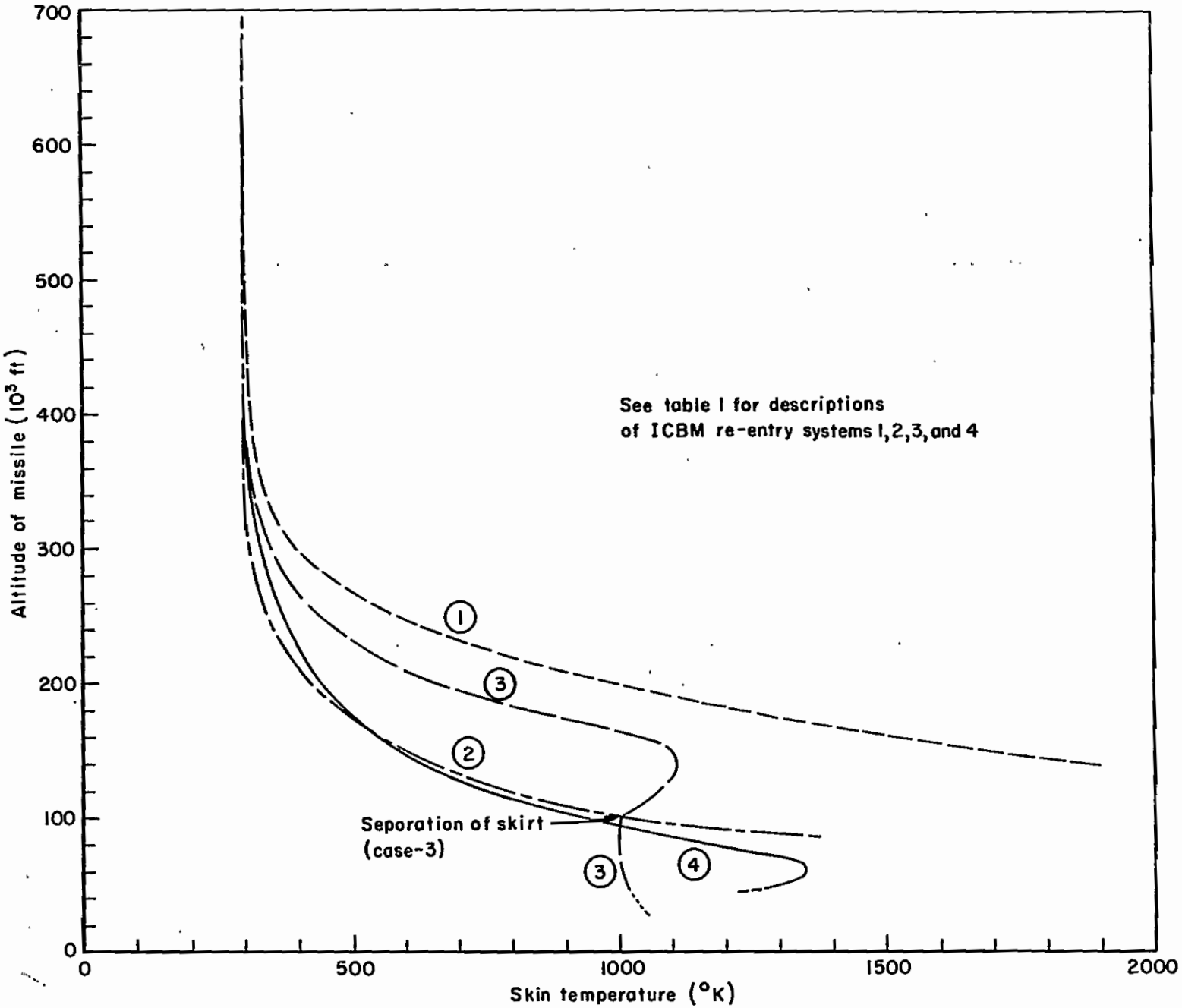

Fig. 1— Frontal skin temperature as a function of altitude for various ICBM systems

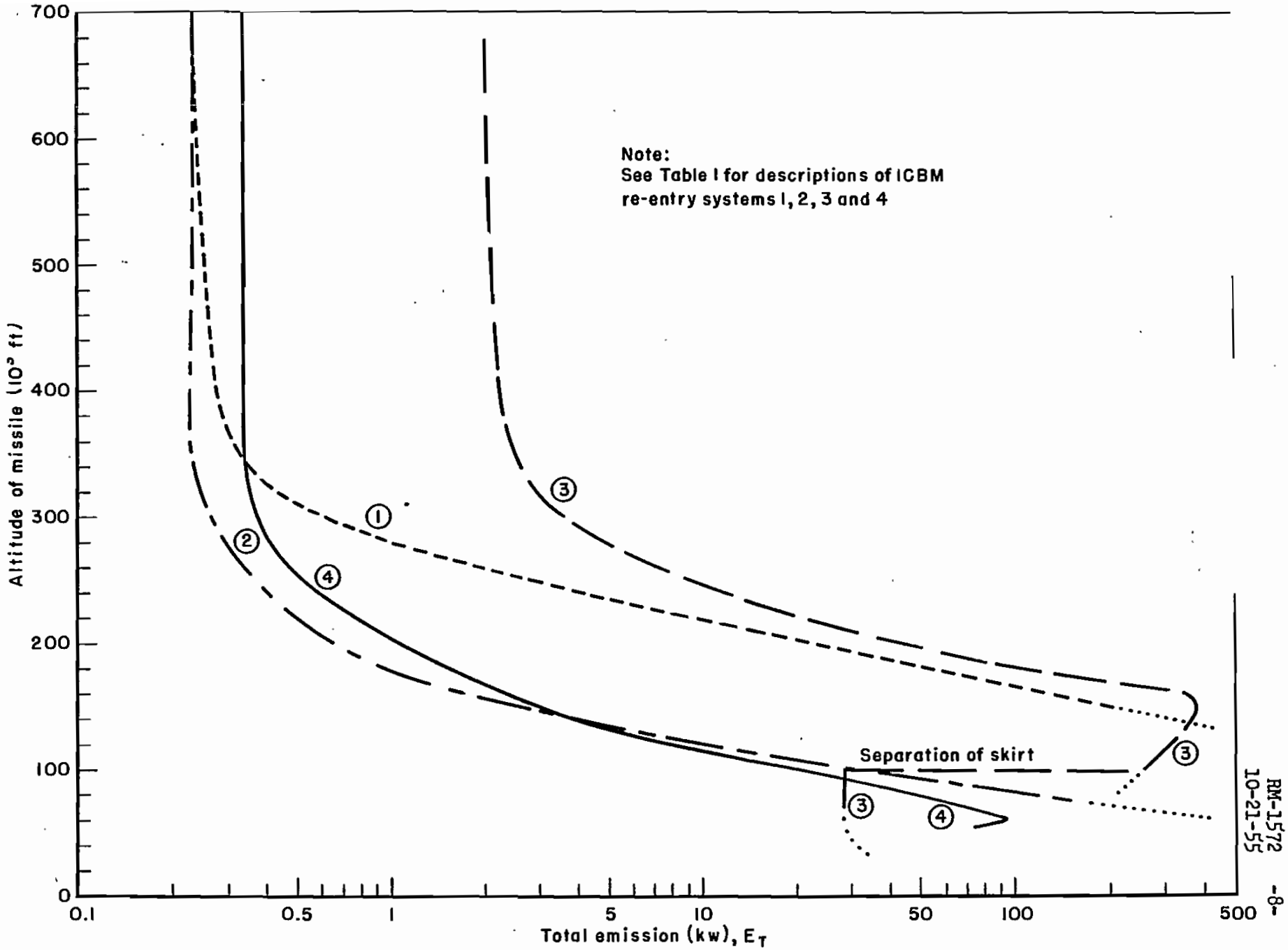

Fig. 2 — Total emission as a function of altitude for various ICBM systems

characteristics given above are somewhat uncertain since they depend on a number of arbitrary assumptions about such factors as the kind and thickness of the missile skin, the kind of flow in the boundary layer -- laminar or turbulent -- and the emissivity of the skin material. There is the possibility that they are generally too low (and therefore conservative for this application) in the lower part of the trajectory (below 100,000 ft), since they are based on calculations assuming laminar flow around the missile. Above 100,000 ft the assumption of laminar flow appears to be reasonable.

The contribution of high-temperature gas radiation (due to shock wave excitation on re-entry) to the emission characteristics of the re-entry body is currently being evaluated. It appears that the radiation from this excited air may be an important factor in the heating of the re-entry body itself at low altitudes if turbulent air flow and its much larger heating rate could be avoided. Estimates of the monochromatic emissivity of air at high temperature indicate that this value may approach unity in the ultraviolet region of the spectrum and may be fairly large in the blue part of the visible spectrum. Photoemissive detectors and multiplier tubes could detect this radiation with excellent sensitivity and spectral efficiency. However, as pointed out by C. Gazley, this gas radiation is expected to increase strongly with air density, velocity of the re-entry body, and radius of curvature of the re-entry body, so that it is most severe for a blunt body travelling at very high velocity at low altitude -- which is indeed an unlikely combination. For the purpose of this discussion of infrared detection at high altitude gas radiation is not considered to be significant.

It is possible to launch the 5,500-mi ICBM on shorter ranges with a considerable variation in re-entry angles. For very high altitudes (greater

than 200,000 ft) it can be shown for a given re-entry velocity that the temperature rise of a thin-skinned re-entry body penetrating to a given altitude is inversely proportional to the sine of the re-entry angle.(3) On page 24 the data of Figs. 1 and 2 will be modified by this relationship in computing infrared detection ranges as a function of re-entry angle and altitude.

C. MINIMUM DETECTABLE FLUX AND SPECTRAL RESPONSE OF THE DETECTION SYSTEM

1. Theory of the Detection System

The maximum target range at which an infrared seeker is expected to yield reliable guidance information is obtained from the basic range equation, Eq. (1). The dependence of P_T, the seeker threshold sensitivity, on the various detection system parameters will now be discussed.

In the near-infrared spectral region, of interest in ICBM-detection applications, the infrared photoconductor detectors offer the most promise because of their high inherent sensitivity and short time constants. The photoconductor current noise is usually observed to be the limiting noise of the detection system. At frequencies below 10,000 cps the detector current noise exhibits a power spectral density inversely proportional to the frequency, f.* Hence, the rms noise voltage in a bandwidth $f_2 - f_1$ is $\sqrt{\log_e f_2/f_1}$. To take advantage of this noise behavior, as well as to discriminate against d-c or slowly varying backgrounds, the infrared signal from the target incident on the detector is made to vary in time by introducing a chopping reticle in the optical system before the detector.

*See R. Clark Jones, Ref. (7), for a detailed discussion of the detection parameters of photoconductors.

Electronic filtering of the detector output is used to limit the effective guidance signal to the optimum frequency region. Since the detector responsivity behaves like a single-time-constant filter, τ_D, the signal output will be proportional to $\frac{1}{\sqrt{1+(2\pi f_s \tau_D)^2}}$, where f_s is the fundamental frequency introduced by the chopping reticle.

Taking these properties into account, together with the optical gain and size effects of the detector system, results in the following phenomenological expression for the infrared seeker threshold, P_T, expressed in <u>effective</u> watts per cm^2 at the seeker aperture.

$$P_t = G\,S\,\frac{\sqrt{A_D}}{A_{eff}}\,\sqrt{1+(2\pi f_s \tau_D)^2}\,\sqrt{\log_e\left(\frac{f_2}{f_1}\right)} \quad \text{watts/cm}^2 \qquad (2)$$

where: G is the minimum signal-to-noise ratio required for effective system operation with a high lock-on probability. This factor may vary from a value of $\frac{1}{4}$ for a pre-slaved gyro-stabilized seeker head as in air-to-air missiles, to about 5 for the case of a displayed scan presentation where the decision of an observer is required. An additional factor of approximately 2 should be included in G to account for field and operational degradation of the system sensitivity. Values of this and other parameters involved in P_T are given in Table 3 for the particular system chosen for this application.

S is the infrared detector's noise equivalent power as measured in the laboratory under the standard reference condition (Jones's quantity "S^n"*). In connection with the definition of detector spectral efficiency given below, the value of S for monochromatic radiation at the wavelength of peak cell response should be used. Values of S for the different detectors are given in Table 2. These values were taken from unpublished data-summary curves of the Naval Ordnance Laboratory, Corona. However, since the NOL values are

*See Ref. (7) for a rigorous definition of "S."

TABLE 2

REPRESENTATIVE CHARACTERISTICS OF SEVERAL TYPES OF PHOTOCONDUCTIVE CELLS

Detector	Wavelength for peak response (microns)	Lower wavelength for 1/2 peak response (microns)	Upper wavelength for 1/2 peak response (microns)	S For monochromatic radiation at peak response wavelength (watts)*	τ_D (μ secs.)
PbS (20°C)	2.1	0.9	2.5	2.5×10^{-10}	350
PbS (-78°C)	2.5	0.9	3.2	4.4×10^{-11}	1,800
PbTe (-196°C)	4.2	<.5	5.0	1.5×10^{-9}	10 - 20
PbSe (-196°C)	5.75	2.75	7.0	7.7×10^{-9}	10 - 20

*Although the dimensions of S are usually given in watts, it is tacitly assumed that the reference condition includes unit detector sensitive area. S consequently has the dimensions watt- cm^{-1}, so that equ. (2) is dimensionally correct.

based upon "the rms value of the fundamental component of the heat signal" it was necessary to increase $S_{(NOL)}$ by the normalization constant $\frac{1}{\frac{\sqrt{2}}{2} \times \frac{2}{\pi}} = 2.22$ so that the equivalent noise input power could be put in terms of the usual full source intensity.

A_D is the detector's useful sensitive area, in cm^2.

A_{eff} is the effective optical aperture area with transmission losses and occlusion of the optical system taken into account, in cm^2.

f_1, f_2, f_s are the upper and lower limits of the amplifier bandwidth and the center chopping frequency of the scanning system, respectively. Scanning system considerations and background discrimination techniques usually dictate the frequencies and bandwidth employed. Design considerations for a seeker for the anti-ICBM interceptor application are discussed below.

η_D is the detection system spectral efficiency, defined as follows:

Let $S_D(\lambda)$ represent the spectral response of the detector as a function of wavelength, normalized so that the peak response is taken as unity, and let $J_\lambda(T)$ represent the spectral radiant intensity of a black body at temperature T; then

$$\eta_D(T) = \frac{\int_{\lambda_a}^{\lambda_b} J_\lambda(T) S_D(\lambda) d\lambda}{\int_0^\infty J_\lambda(T) d\lambda}$$

where λ_a and λ_b represent the limits of the filtered wavelength region used with the detector. Characteristic values of $\eta_D(T)$ are given in Fig. 3 for several infrared detectors. For PbS and PbTe a filter with 0 transmission up to 1.4 μ and unity above this wavelength is assumed present in the system for background discrimination purposes, as discussed on page 26.

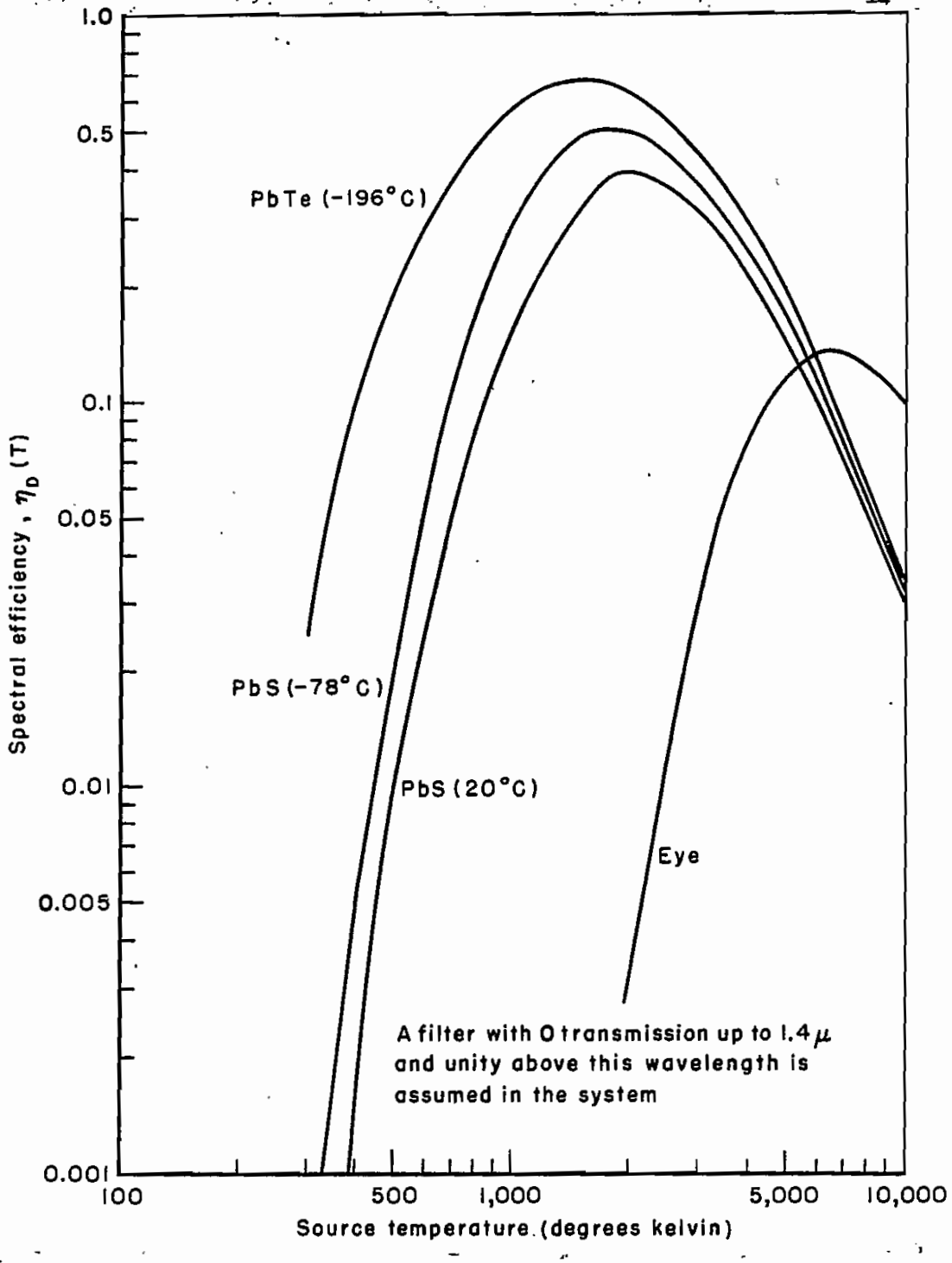

Fig. 3 — Detector spectral efficiency as a function of source temperature (for PbS and PbTe)

2. Requirements on the Detection System

For a detailed evaluation of the threshold sensitivity, P_t, and the maximum infrared range, R_{max}, the seeker characteristics must be considered in terms of the particular application, which in this case is the terminal guidance phase of an interceptor missile. To make the discussion specific, the infrared guidance is assumed to be operated in conjunction with a system of the "one-eyed goalie" type[8][9], used for interception at altitudes greater than 100,000 ft. The intercepting missile is guided along the initial phase of its trajectory by radar*, and the infrared seeker is pre-positioned to the approximate direction of the line of sight to the re-entry vehicle.

Since the infrared seeker is envisaged as operating above the dense, moist part of the atmosphere, the transmission factor, η_w, is assumed unity in the spectral region of interest here. The usual air-to-air missile infrared seeker design characteristics aimed at minimizing the background signal due to clouds, horizon, and sky gradients need not apply in this application, although it is shown below that the utilization of a spectral filter with a lower wavelength cutoff at about 1.4 μ will be very helpful in essentially eliminating the star background.

a. Resolution (Angular Accuracy) and Time of Acquisition. It is conceivable that with very accurate mid-course guidance, the only guidance information needed from the infrared seeker would be notice that an angle threshold was exceeded by the line of sight to the re-entry body. This information could serve to fuze the defensive weapon. However, the more

*See Ref. (4) for a discussion of the radar tracking problem.

complex guidance requirement of line-of-sight rate information will be treated. Such information could serve to place the intercepting missile along a transverse collision course with the ICBM, under the control of some auxiliary rocket propulsion system (as in the one-eyed goalie type of interceptor).

In this application, because of the limited thrust capabilities during the terminal phase of the intercepting missile and the very high closing velocities (as high as 23,000 ft/sec at altitudes greater than 150,000 ft), the required detection ranges are formidable, i.e., 20 to 40 miles. With this large a detection range and with an assumed initial deviation of the order of 1 mile from the trajectory of the incoming missile, it is found that the excursion of the line of sight from its initial position during the interception is less than 1.5 degrees. For this reason, if the seeker is positioned accurately enough under ground control and if it is stabilized during midcourse, it may not be required to track the target but only to observe the rate of change of the line of sight and to sense the null in the line-of-sight rate indicative of a collision course. The required angular resulution of the infrared seeker is determined by the minimum line-of-sight rate confusable with a null condition, which in turn depends on considerations of miss distances compatible with the lethal radius of the defensive weapon[4] together with the system response time. The principal component of the system response time is the reaction time of the propulsion control system. For the "one-eyed goalie" high-altitude interceptor the resolution requirement is about 1 minute of arc.[8][9]

b. System Bandwidth. Information regarding the line of sight to the target can be obtained in analog form by coding the seeker focal plane with

a reticle and observing the modulated signal output of the detector. An amplitude-modulated signal can be produced simply by rotating a spoked chopper which also has a uniform transmission gradient across the reticle. A frequency-modulated signal can be obtained by rotating the optics off axis in conjunction with a spoked chopper. Modulation techniques of this kind are familiar from methods explored in conjunction with infrared seeking air-to-air missiles.(10)(11)

The a-m system has an important advantage for this application by offering a linear dependence of modulation coefficient upon angular deviation of the target's line of sight from the center of the pattern over the entire field of view. The phase of the demodulated wave can be made to correspond to the sense of the target's position relative to some body axes, so that the error signal can be resolved into a reference co-ordinate system. Electronic differentiation of the above resolved error signals yields direct information on the line-of-sight rates, and the null is detected accordingly.

A disadvantage of the a-m system is the requirement of an automatic gain-control circuit to avoid saturation of the signal amplification stages, in view of the great increase in infrared flux in the course of the interception. The very large range closure rate (as great as 23,000 ft/sec at high altitude) requires that this AGC system have a short time constant, approximately 0.01 sec. The action of this AGC will be to keep the mean rectified carrier level constant. In order to prevent degradation of the information at the modulation frequency, this latter frequency, essentially the scanning rate of the infrared seeker, must be kept high, of the order of 200 cps.

This determines the minimum amplifier bandwidth required as approximately 500 cps, centered around the carrier frequency. The carrier frequency may be

chosen as the optimum detector chopping frequency, given by

$$f_s = \frac{1}{2\pi\tau_D} \quad \text{cps} \tag{4}$$

Therefore,

$$f_1 = 250 + \frac{1}{2\pi\tau_D} \quad \text{cps}$$

$$f_2 = \frac{1}{2\pi\tau_D} - 250 \quad \text{cps}$$

c. Size of Cell and Optics. The remaining terms in (2) needed to evaluate the seeker threshold sensitivity, P_t, are the effective aperture area and detector sensitive area. In the design of the seeker for the ICBM interceptor it appears possible to allow a diameter of approximately 25 cm. Assuming a factor of 40 per cent for a reasonable optical efficiency, due to occlusion of a Cassegrain reflective optical system, which might be employed, and due to transmission losses in the scanning reticle and other optical elements, an effective aperture area of 200 cm^2 can be considered. Because this application requires terminal infrared guidance to be effective only above 100,000 feet and because the velocity of the defensive missile would be rather low at this stage, the irdome problem does not appear to be serious. In fact, the severe requirements on angular accuracy may make it worth while to consider dispensing with a seeker window. Any protective cover used during the boost stage might be shed at the time of booster separation.

The minimum detector size for the aperture given above and the required half-angle field of view of approximately 2°, is determined by the optical sine condition. This results in the choice of a detector area of 4 mm by

4 mm, assuming immersion of the detector in a medium with refractive index intermediate to that of air and that of the detector itself.

The choice of field of view above was based on preliminary estimates of the accuracy with which the seeker could be pre-positioned to the target direction. If it is necessary to have a search phase prior to the guidance phase, this can be accomplished by nutating the seeker head within a radius of 1.5°, allowing complete coverage of a sector of space of 7° total angular extent. Although the search would have to be done as rapidly as possible, the nutation rate would have to be slow enough so that the motion of the field during the time needed for signal detection and the time needed to de-activate the nutation would not be a significant part of the instantaneous field. A scan rate of the order of 1 cps might be reasonable.

In order to have a low false-alarm rate during the search process a higher signal-to-noise ratio threshold would be required so that G (see Eq. (2)) would be increased from a value of 4, as assumed for the guidance phase, to about 8 for the search phase, decreasing the maximum detection ranges given in Section D, below, by 30 per cent.

The above seeker design characteristics are summarized in Table 3. These, together with values of S and τ_D given in Table 2, when introduced into Eq. (2), result in the following values for P_t, the threshold sensitivity of the infrared seeker:

Seeker employing uncooled lead sulfide detector

$$P_t = 3.1 \times 10^{-12} \text{ effective watts/cm}^2$$

Seeker employing lead telluride detector

$$P_T = 3.3 \times 10^{-12} \text{ effective watts/cm}^2$$

TABLE 3

ICBM INTERCEPTOR INFRARED SEEKER DESIGN CHARACTERISTICS

Diameter of seeker	10 inches
Effective aperture (A_{eff})	200 cm^2
Instantaneous semi-field of view	2 degrees
Detector size	4 mm x 4 mm
Scan system	rotating reticle - amplitude modulation type
Electronic bandwidth ($f_1 - f_2$)	500 cps*
Chopping frequency (f_s)	A. Uncooled lead sulfide system 500 cps B. Lead telluride system 7,500 cps
Minimum S/N (G)	4
Spectral filtering	lower wavelength cutoff at 1.4μ, upper limit determined by detector response

*The one-eyed goalie's response time of about 0.1 sec. would imply that the minimum theoretical signal bandwidth in this application would be of the order of 10 cps. With the amplitude-modulation scanning system chosen for its important linear properties over the entire field, AGC considerations, as well as reticle positioning problems require a bandwidth as given above. This same engineering compromise is made on infrared seekers for present air-to-air missiles. As seen from Eqs. (1) and (2), any reduction in required bandwidth would reflect itself in an increase in detection range approximately proportional to the fourth root of the bandwidth ratio.

D. MAXIMUM DETECTION RANGES DURING RE-ENTRY

Using the values of re-entry body emission, E_T, and surface temperature, T, given in Figs. 1 and 2 as a function of altitude, and the detector spectral efficiency given for these temperatures in Fig. 3, together with the threshold sensitivity given on page 19, determines the maximum infrared detection range of the seeker for the one-eyed goalie type of anti-ICBM interceptor. The data are plotted as a function of the altitude of the re-entry body in Fig. 4.

Infrared detection ranges are given for seekers employing uncooled lead sulfide, and lead telluride detectors. Since the ranges for a lead sulfide system are approximately only a fourth as large as those for lead telluride it appears necessary to use a lead telluride or other long-wavelength-sensitive detector for this high-altitude interception application. This will involve the complication of maintaining the PbTe detector at a very low temperature (-195° C), to obtain the necessary sensitivity. However, recent advances in miniaturized cooling equipment appear to make it possible to satisfy this requirement for the short guidance times involved in this application.

For the type of interception described above, a more meaningful calculation is that which determines the time available from first infrared detection of the re-entry body to its falling to the interceptor's altitude, as a function of the interception altitude. This time has also been calculated as a function of ICBM re-entry angle and velocity, and the results are given in Figs. 5, 6, 7. It appears from studies now in progress at RAND that these infrared guidance times may offer adequate action time for the interceptor missile to reduce the original miss distance to within the lethal radius of its warhead.

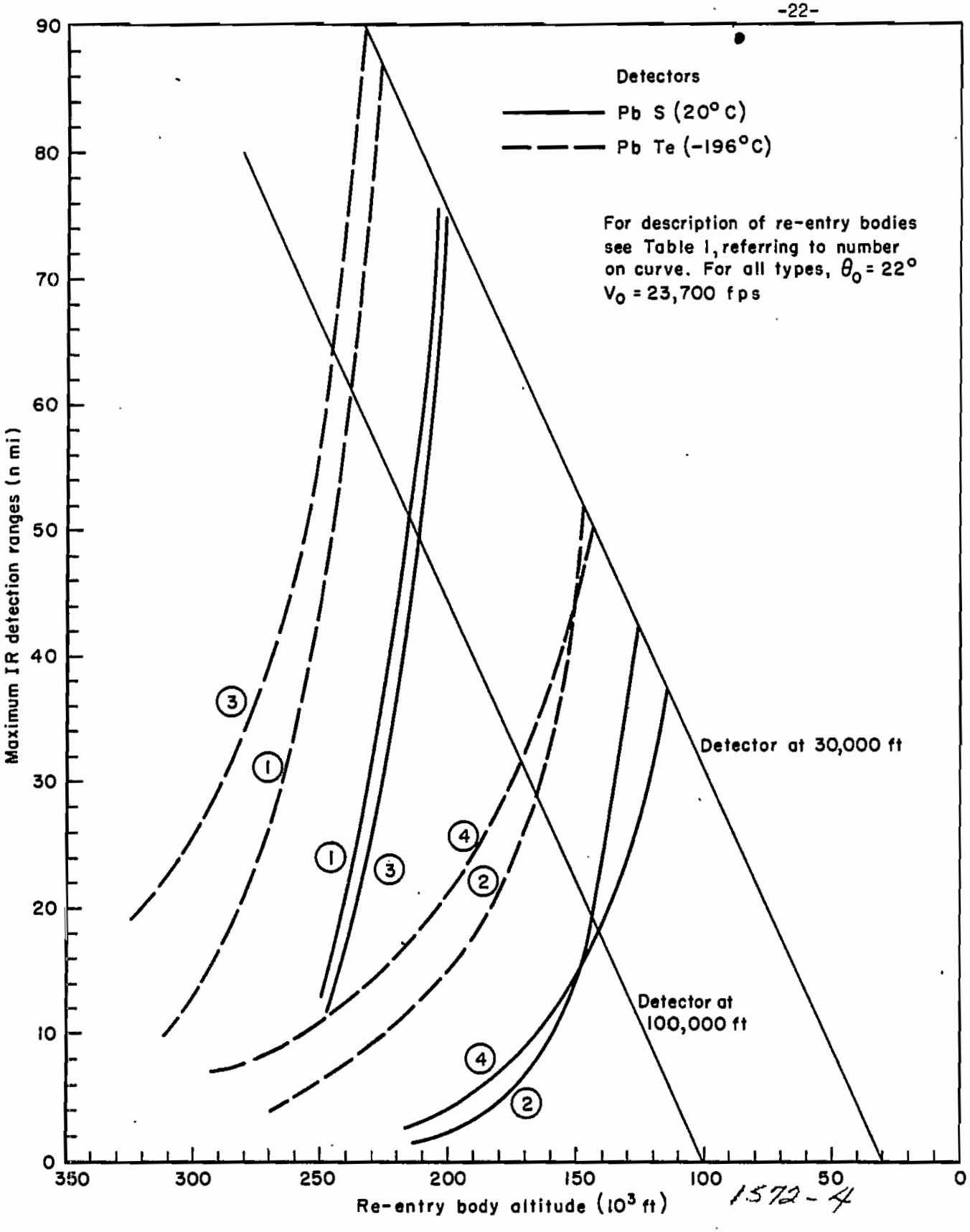

Fig. 4—Maximum IR detection ranges on various re-entry bodies

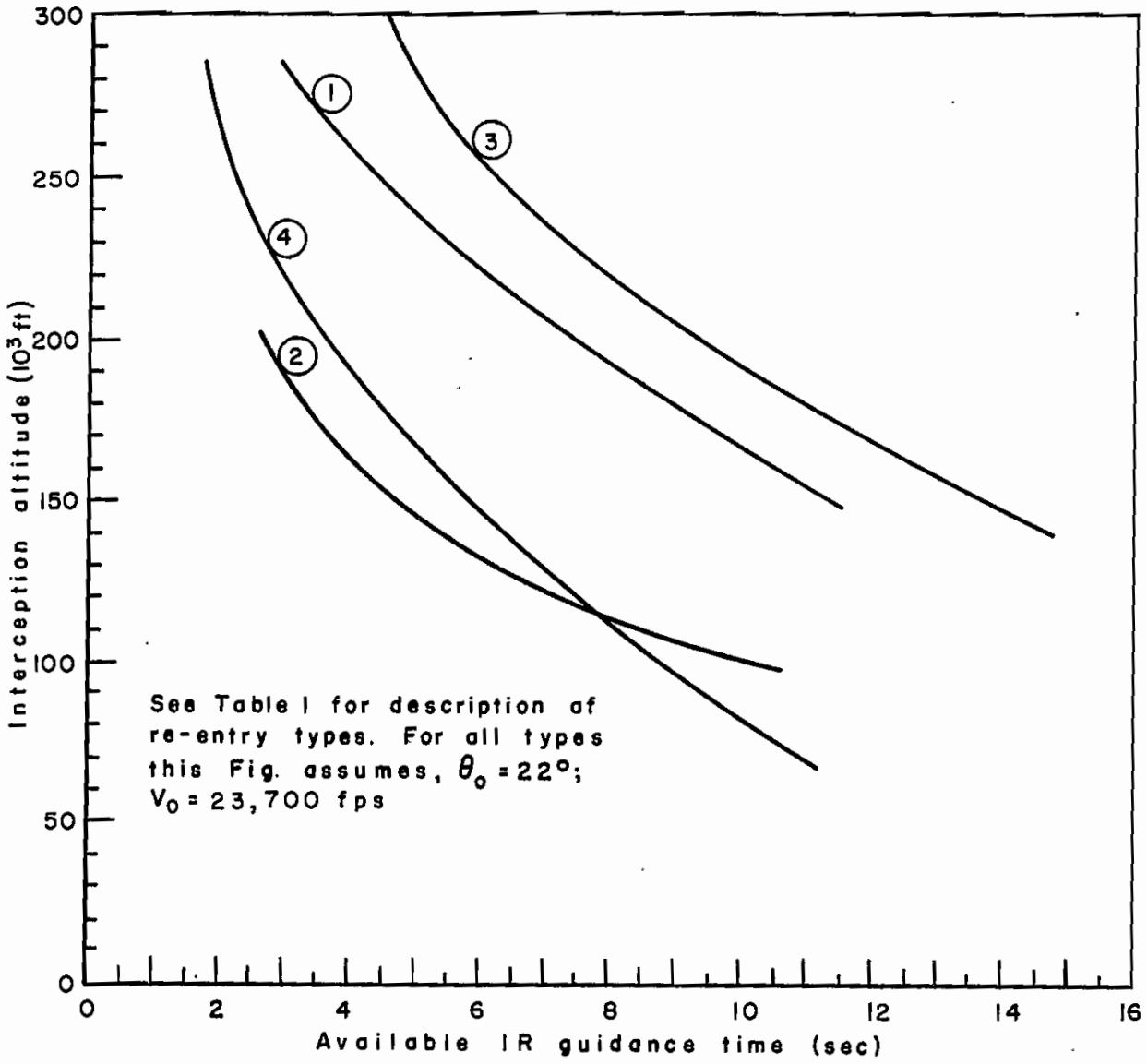

Fig. 5 — Maximum available IR guidance time as a function of interception altitude 1572-4

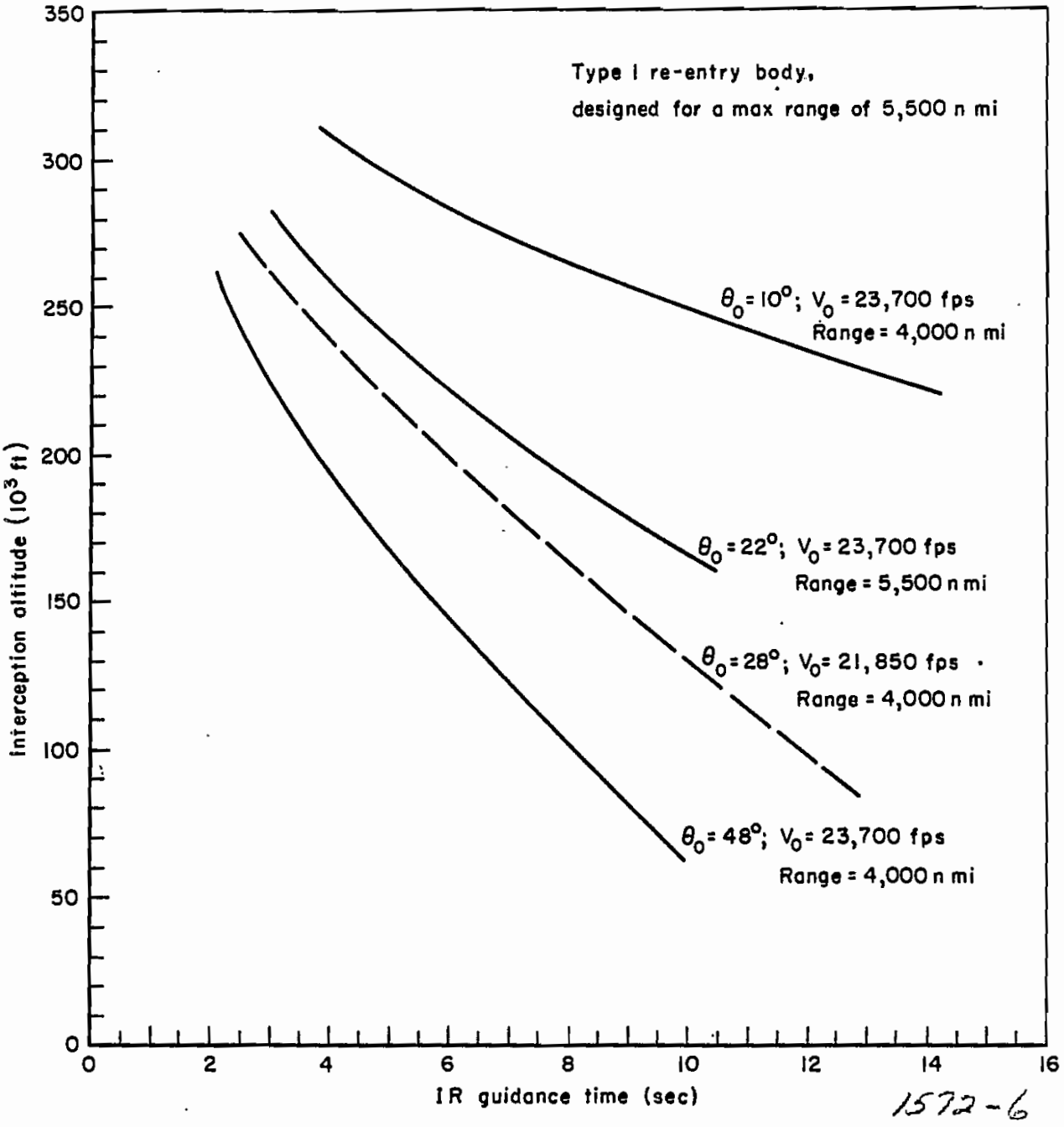

Fig. 6 — IR guidance time dependence on re-entry angle and velocity

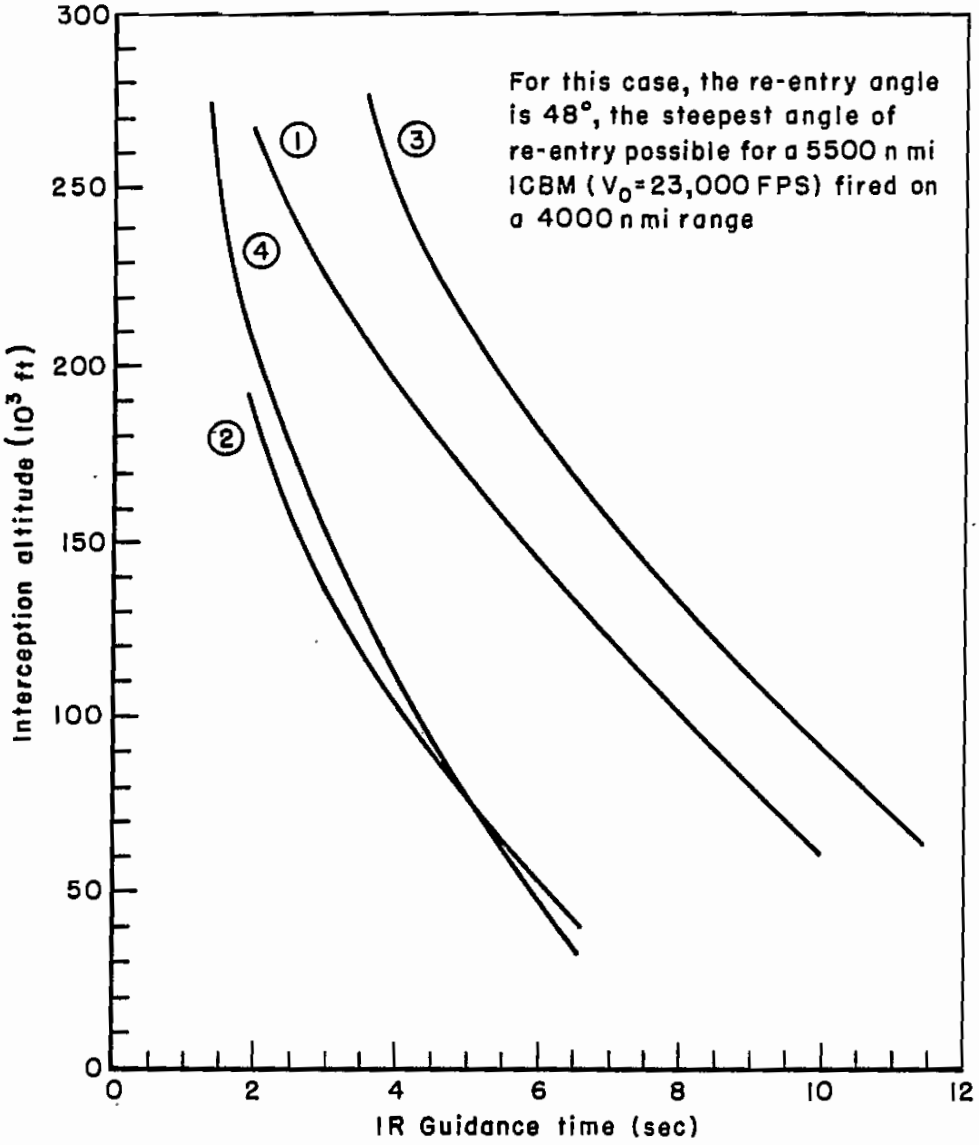

Fig. 7 — IR guidance time vs interception altitude
See Table I for description of re-entry bodies

E. DISCRIMINATION AGAINST THE STAR BACKGROUND

Although the usual disturbing infrared backgrounds of horizon, clouds, and sky gradients will not be observed in the very-high-altitude interception application, it is necessary to consider the background due to radiation from celestial objects and meteors.

Available information on the visual magnitudes of stars, together with estimates of their radiation temperatures, can be used to determine the infrared flux reaching the seeker in its spectral region of sensitivity, after the method outlined by L. Larmore.(12)

From the definitions of visual magnitude and spectral efficiency of the eye and the infrared detector, it follows that the effective infrared radiation incident on the seeker from a star of visual magnitude M_1, and temperature T, is:

$$\dot{E} = 3.37 \times 10^{-13} \times \frac{\eta_D(T)}{\eta_{eye}(T)} \times 10^{-0.4M_1} \text{ effective watts/cm}^2 \qquad (5)$$

Values of $\eta(T)$ for the eye, and for PbS and PbTe are given in Fig. 3. Here, the lower limit of accepted wavelength for the infrared seeker has been chosen as 1.4μ so as to filter out the greatest part of the radiation from the very hot celestial objects, while very little of the radiation from the relatively low-temperature re-entry body is lost by this technique.

A list of those celestial objects that emit sufficient infrared radiation to be possibly detectable by the infrared seeker described above is given in Table 4. (Note that the limit set here is actually about two-thirds that of the threshold for the infrared system, P_t, so that some of the celestial objects in Table 4 would probably not be detected.) While a

balanced chopper[13] might be employed to discriminate further against these sources of high effective temperature, the small number of interfering objects and the very small field of view of the proposed seeker make the probability of lock-on for a star or planet so small that it does not appear worth while to go to this degree of sophistication.

TABLE 4

Celestial Objects Whose Effective Radiation Exceeds 2×10^{-12} watts/cm^2

Effective Radiation at the Seeker Aperture

(with a 1.4μ lower wavelength cut-off filter)

Celestial Object	Intensity (effective watts/cm^2)	
	PbS System	PbTe System
Sun	1.2×10^{-2}	1.5×10^{-2}
Moon (full)	2×10^{-8}	2.5×10^{-8}
Jupiter (at brightest)	2.1×10^{-12}	2.7×10^{-12}
Mars (at brightest)	2.1×10^{-12}	2.7×10^{-12}
Venus (at brightest)	1.4×10^{-11}	1.7×10^{-11}
Betelgeuse	2.2×10^{-12}	3.0×10^{-12}
Mira	2.8×10^{-12}	3.9×10^{-12}

F. METEORS, A NATURAL DECOY

A calculation was made to determine the probability that a meteor of intensity great enough to be detected by the infrared seeker would cross the field of view of the seeker during the time of guided interception of the re-entry body.

Meteors, due to their extremely high entry velocity, become heated at considerably higher altitudes than the re-entry body.* Their average height of visual appearance is approximately 60 miles. Because of their high velocity and small size they disappear as the result of vaporization at an average height of 50 miles.

Assuming an average temperature of the luminous meteors of approximately $3{,}500^{\circ}$ K, and taking into account the different spectral efficiencies of the infrared detector and the eye as in the previous section, it is found that only meteors of visual magnitude of unity or less (i.e., brighter than magnitude one) will yield an intensity exceeding 1.8×10^{-12} effective watts/cm^2 to the lead telluride detector seeker system.

There are, on the average, about 3×10^6 meteors of visual magnitude less than unity entering the earth's atmosphere each day. (There are considerably more than this during the very limited periods of meteor showers.) Assuming a seeker field of view of 4°, an interceptor altitude of 150,000 and a seeker sensitive time of 15 secs, only 1.4×10^{-10} of the total number of meteors entering the atmosphere are likely to be found in a region of space and time observed by the infrared seeker. This results in a probability of responding to a meteor track during interception of 1 in 2,500, which is probably considerably less than the abort rate expected for the interceptor vehicle.

*The authors have profited from discussion with Dr. H. Kallman, RAND consultant, concerning meteor properties.

III. CALCULATION OF MAXIMUM DETECTION RANGES DURING TAKE-OFF OF AN ICBM

There are three chief differences between the detection operations during re-entry and those during take-off of the ICBM:

- During the ICBM boost period, the time for viewing the missile is much longer, so that slower (more sensitive) cells can be used.
- During the actual boost, while the rockets are firing, there may be strong emission of infrared by the rocket flame as well as by the heated skin. Preliminary calculations and observations at sea level indicate that some of the exhaust gases will emit strongly at certain infrared wavelengths, within the sensitivity range of PbS and PbTe cells, but that the intensity of the rocket emission will decrease with altitude.
- The higher temperature of the rocket exhaust gases permits the use of shorter wavelength IR detectors such as lead sulfide in this application. Advantage can be taken of their better inherent sensitivity while still maintaining high spectral efficiencies at these high color temperatures.

In the following paragraphs the problems of infrared detection of an ICBM during take-off will be investigated, and estimates of maximum detection ranges will be presented. A specific context will be taken as the basis for the analysis: the detection equipment will be assumed to be carried by an aircraft patrolling outside the borders of the Soviet Union. A look at the map shows that no place in the Soviet Union is more than about 1200 n mi from a Soviet border. With this figure in mind, the question to be considered is: Can airborne infrared equipment detect an ICBM taking off from

a launching site at ranges up to 1200 n mi? Figure 12 shows what the relative position of missile and search aircraft might be.

A. ICBM EMISSION DURING TAKE-OFF

While the actual characteristics of the ICBM to be detected during take-off are to be determined by the enemy, it appears that there are certain basic constraints on his choice. For a 5000- to 6000-nautical-mile range the take-off of a two-stage missile is probably fairly well described by Table 5. This is based on calculations assuming an initial thrust-to-gross-weight ratio, η_1, of 1.5, which is considered rather low. If a larger value were used, larger rockets would be required, the powered phase would be shorter, burnout would occur at a lower altitude, and the skin temperature would be higher because of the greater velocity attained while the missile is still in the lower atmosphere. In other words, the emission during take-off would be even greater than for the $\eta_1 = 1.5$ case, but it would not last as long.

It seems likely that multiple rockets may be used, probably three or four, to give the large thrust required for the first stage, and that a single rocket may be used in the second stage, with a somewhat smaller thrust but a larger expansion ratio (the ratio of the nozzle exit area to the throat area) in the nozzle, to compensate for the near-vacuum in which it is intended to operate. At any rate, it will be assumed that this is the case, and that the rocket nozzles will all have an exit diameter of the order of one meter.

The missile itself will be considered to have dimensions (in round numbers) as follows: Initial length of body, 30 m; diameter, 3 m; length of body of second stage after separation, 6 m; conical warhead extending

Table 5

ICBM TAKE-OFF CHARACTERISTICS*

Altitude (10^3 ft)	Time from Take-off (sec.)	Stage which is Firing	Daytime skin Temp. (°K)
50	66	First	375
100	90	"	520
200	120	"	575
400	165	Second	520
600	205	"	475
800	245	"	435
1000	280	"	400
1500	365	None	370

*Prepared by Carl Gazley and Hans Lieske, RAND Missiles Division.

forward from body, base diameter 1.5 m, length 2 m. For a further description, see Ref. 4.

So far, the rocket and missile itself have been described closely enough for the purpose of this investigation; it is also necessary to describe the infrared emission from the flame behind the rocket. At sea level, it is possible to get a rough estimate of the emission from such a rocket flame by observation of test stand firings. Observations of smaller rocket motors, below 1500-lb thrust, indicate the following:(14,15,16)

Acid-aniline flames emit a continuum in the visible on which are superimposed weak band systems due to NH and CN. The spectrum in the visible can be described roughly as that of a grey body, with an emissivity of

.0055 to .006 and a temperature of about 2700°K. In the infrared, considering the total emission as detected by a pyrometer, the emissivity appears to be some three times greater, assuming the same effective temperature of about 2700°K. Thus, if the temperature of the flame were 2700°K, the infrared or total emissivity is about .02; if the effective temperature were about 2000°K, as it is in certain parts of the flame, the equivalent total emissivity is about .06.

Alcohol-liquid-oxygen flames emit discrete lines and bands in the visible, superimposed on a relatively weak continuum. The lines and bands observed have been identified as those of Na and CaO (presumably from impurities in the fuel), OH and CH. Although no spectral observations in the infrared for alcohol-oxygen or jet-fuel-oxygen flames appear to have been made, it is known that the combustion products of these fuels are molecules which have thermally excitable bands in the near and middle infrared. Therefore, one would certainly predict some emission in the 1 to 5 micron region, probably as much as for the acid-aniline flame.

Finally, high-speed color movies of test stand firings of large rocket motors (over 100,000 lbs thrust) using jet fuel and liquid oxygen show that the flame as it first leaves the exit is a blue-green color, with relatively little continuum--as mentioned above for the alcohol-liquid-oxygen flame. However, starting a meter or two from the nozzle there is a brilliantly glowing mantle, which appears to begin as a surface emission and become diffused throughout the flame at greater distances from the nozzle. The spectrum of the mantle is a continuum with weak band systems superimposed. The explanation of this mantle is probably to be found in the fact that such motors run on a rich mixture, and the hot exhaust gases react with the air,

causing a further combustion. The bright continuum is then due to this interaction of the air with unoxidized carbon, and the result is analogous to the glow of a candle. Tests with smaller rockets have clearly demonstrated the very marked difference between the emission from a lean mixture and a rich mixture, so there can be little doubt about the general cause of the mantle or candle effect. The significant factor to bear in mind is the need for a reaction with the ambient air to produce this very intense continuum. At altitudes encountered during the last part of the powered flight it is likely that the effect of the mantle will markedly decrease.

Another change will occur as the rocket moves to greater altitudes. A rocket flame, firing at sea level, always displays a succession of bright spots along the axis of the flame. These are sometimes clearly seen as diamond-shaped areas formed by an intersection of shock waves[14][16]--hence the term "Mach node" or "Mach diamond." These are produced by a complicated interaction between the various parts of the exhaust flame, the rocket nozzle, and the ambient air, and may be thought of as standing shock waves formed by a series of reflections from the boundary between the air and the exhaust. Behind these shock-wave intersections the temperatures and pressures are even higher than at the nozzle exit (pressures of 2.5 to 3.0 atmospheres, temperatures over 2600°K), and the resultant thermal emission is therefore quite strong from these regions. Here again, in the absence of air at high altitude the rocket flame would change its shape. General considerations indicate that the Mach diamonds will disappear and that only the first Mach cone will remain.

The implications of these changes to the emission are not entirely clear, but it seems certain that in a vacuum the exhaust gases <u>will not emit as much as they do at sea level</u>, since (a) the mantle will diminish

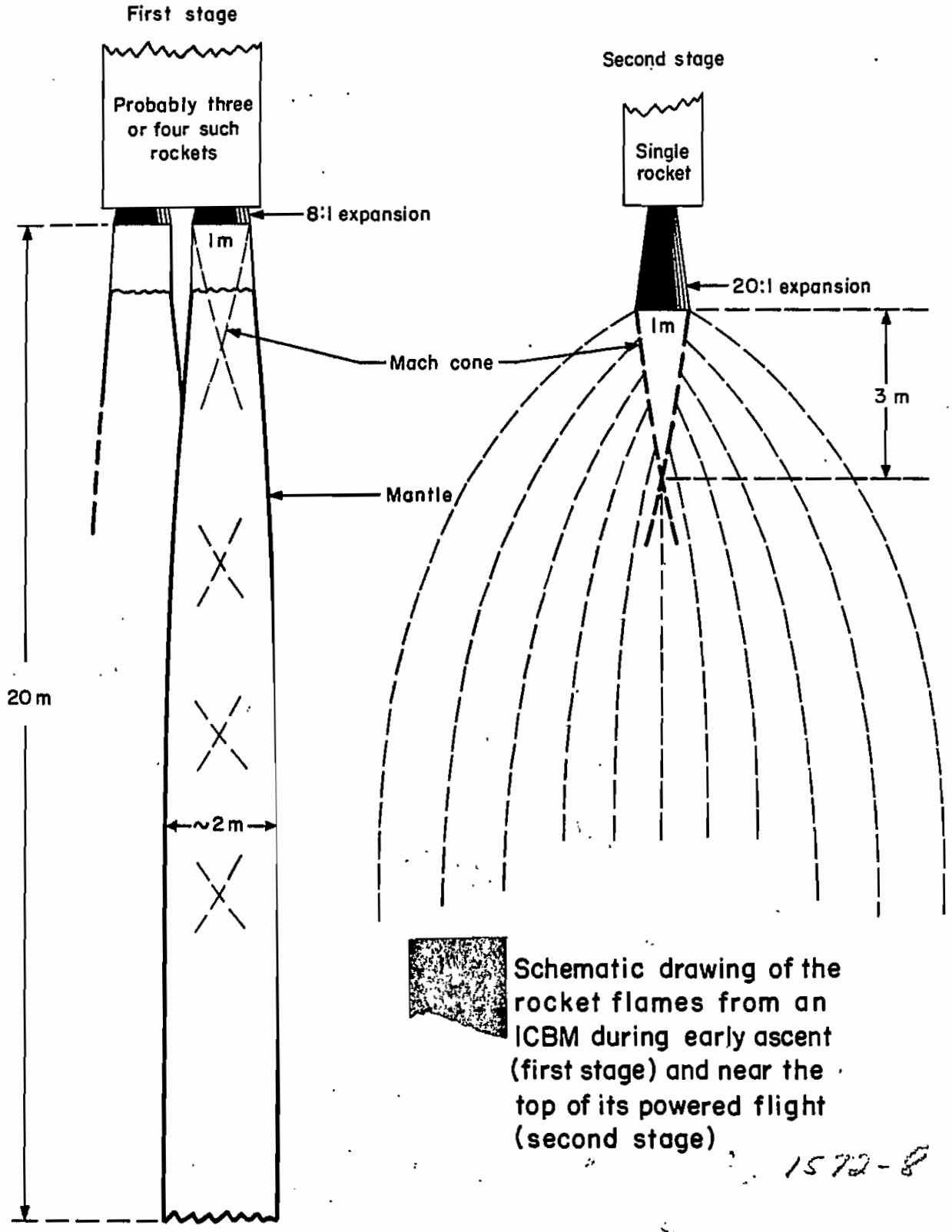

Schematic drawing of the rocket flames from an ICBM during early ascent (first stage) and near the top of its powered flight (second stage)

1572-8

or disappear entirely, and (b) the Mach diamonds with their high temperatures and strong emissions will also disappear. One might consider that a part of the energy which goes into radiation at sea level will go into adiabatic expansion 100 miles up.

With these general considerations in mind, Fig. 8 serves to describe the kind of rocket flame which one would expect from an ICBM at take-off and during the latter part of its powered flight. The second-stage rocket has a thrust which is about two-thirds that of the first stage rockets, but a larger expansion ratio.

At sea level the rocket emits over its whole area as a grey body at 2400°K, having an emissivity of 0.1. (It is assumed that it is running on a rich fuel mixture and that the mantle has a temperature roughly equal to that which would be attained by complete combustion of the fuel at a pressure of one atmosphere. This temperature is a little less than that observed in the Mach diamonds, where the pressure is several atmospheres.)

At high altitude the rocket emits radiation from the Mach cone only, since the rest of the flame cools so rapidly by expansion. Here in the Mach cone the temperature is about 2100°K, and there is only line and band emission due to thermal excitation of the incompletely oxidized combustion products. This should really be treated, therefore, as a discontinuous spectrum, but until better information can be obtained either theoretically or experimentally it will be assumed that in the infrared the emission from the Mach cone is that of a grey body with 0.1 emissivity.

It will be noted that the emissivities chosen are something like two to five times greater than those quoted for the observations of small rocket flames. This is to take into account the increased size and depth

of the large rocket flame, which is about ten times larger in every dimension. It must be remembered also that these emissivities apply to the infrared beyond about 1 μ, emissivities in the visible being less.

The total emission from an ICBM during take-off and boost is summarized in Table 6. The dimensions of the missile are approximately those given by Graham[4]. The view of the missile from the forward quarter (at an angle of 45° from the axis) may be considered as corresponding to the situation during the latter stages of the boost, when the missile is starting on its elliptical trajectory and is viewed from a station near the horizon in the direction of its travel, i.e., a detection station or aircraft at the border of enemy territory. The skin temperatures are taken from Table 5 above, and the emissivity of the skin is taken to be 0.8, which is roughly representative of oxidised steel and a variety of other possible surfaces.

Table 6

TOTAL EMISSION OF AN ICBM DURING ITS POWERED FLIGHT

Altitude (1000 ft)	Skin Temp. (°K)	Flame Temp. (°K)	Side Aspect				Forward Quarter			
			Skin		Flame		Skin		Flame	
			Proj. Area (m^2)	Emission (kw)	Proj. Area (m^2)	Emission (kw)	Proj. Area (m^2)	Emission (kw)	Proj. Area (m^2)	Emission (kw)
50	375	2400	90	83	80	15,000	65	60	55	11,000
200	575	2300	90	430	50	8,000	65	310	35	5,700
400	520	2200	20	68	10	1,300	14	48	7	920
800	435	2100	20	31	1.5	160	14	22	1.0	100
1000	400	2100	20	24	1.5	160	14	16	1.0	100
1500	370	-	20	15	-	0	14	10	-	0

The transition of the flame from the sea-level (or 50,000 ft) characteristics to the high-altitude characteristics is taken rather arbitrarily, since it is not known how fast this occurs. Therefore, the flame emission at each altitude must be considered as an estimate in which an attempt has been made to be on the conservative side, i.e., to underestimate the emission. There are many uncertainties involved, most of which have been enumerated already. In addition, if the missile configuration were such that a part of the rocket nozzle were exposed, the emission from this hot body would be a large addition to that shown.

B. GEOMETRICAL LIMITATIONS ON DETECTION RANGES DUE TO CURVATURE OF THE EARTH AND THE TRAJECTORY OF THE MISSILE

For a very strong radiation source at high altitudes such as a rocket flame or a hot missile skin and a sensitive radiation detector in an aircraft, the limiting range for detection may be determined by geometrical considerations alone. The geometry of the situation involves a number of factors:

- The curvature of the earth.
- The height of the effective horizon, which may be determined by the altitude of the top of a deck of clouds or a mountain range.
- The missile (source) altitude.
- The aircraft (detector) altitude.
- The refraction of the rays by the earth's atmosphere.
- The horizontal motion of the missile

Although all of these factors must be taken into account to compute the maximum range for a given set of conditions, it is possible to generalize

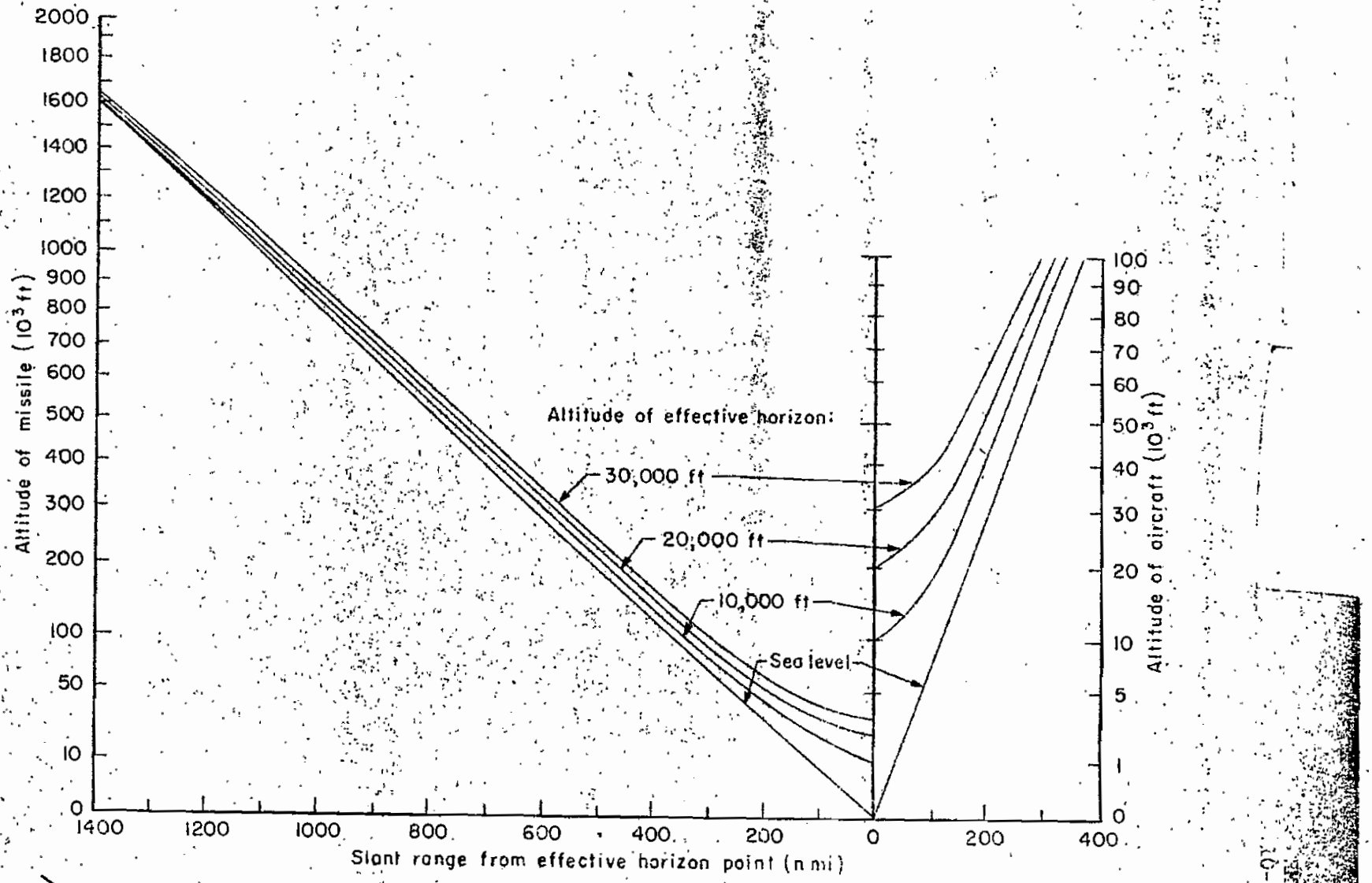

Fig. 9 — Slant range to the effective horizon for a given set of observer and target altitudes

AS-72-57

A-1572
10-21-55
-38-

the problem in such a way that the computations can be done once for a representative range of conditions. The results of such a general solution are shown in Fig. 9.

In arriving at the values shown, refraction of the rays by the atmosphere is the most difficult factor to take into account. However, when refraction is taken into account it does not affect the results by more than about ten per cent (at the most) and in many cases is quite trivial. However, it is important to include it, if for no other reason than to answer questions about the magnitude of the effect of refraction.

If, for the moment, the effect of refraction is neglected, it can be seen by inspection of Fig. 10a that the geometrical range from the point M to the horizon point, H_o, is given by

$$R_g = \sqrt{(\rho + h_m)^2 - \rho^2}$$

$$\cong \sqrt{2\rho h_m + h_m^2} \qquad (6)$$

If refraction is actually occurring, however, a ray from M will be bent in passing down through the atmosphere, and for the case when h_m is very large the added distance to the true horizon point, H, is very nearly $\rho\alpha$, so the optical range is (see Fig. 10b):

$$R \cong R_g + \rho\alpha$$

$$= \sqrt{2\rho h_m + h_m^2 + \rho\alpha} \qquad (7)$$

where the angle α is the angular correction to a ray from an infinite point source (like a star) when it is seen just on the horizon.

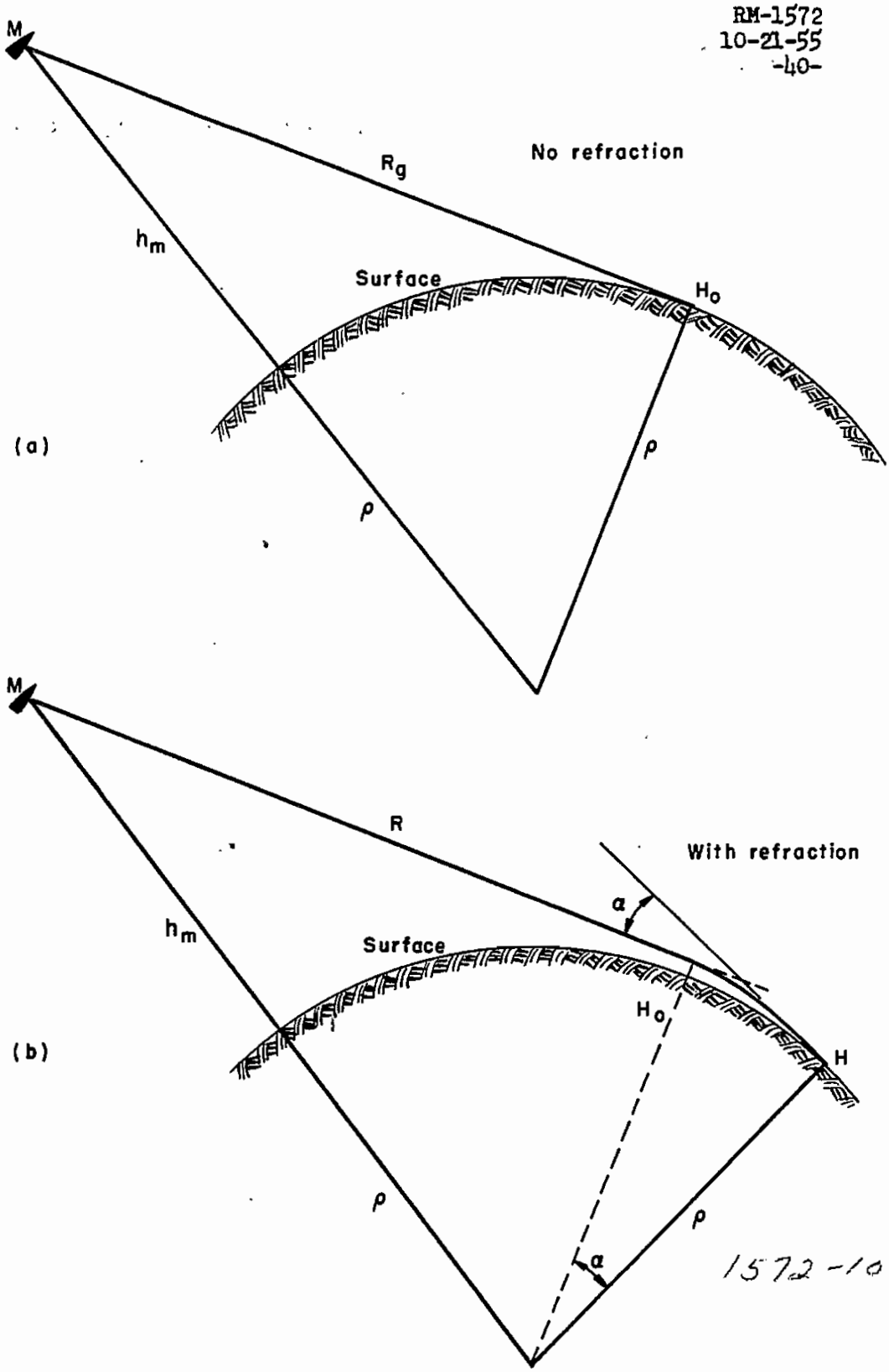

Fig. 10 — Diagrams of the ray geometry for the case of no refraction (a) and with atmospheric refraction (b)

There is an added complication when one considers that the effective height of the horizon point is probably not actually at sea level. Clouds usually determine where the horizon is, and the tops of these layers of clouds may range from ten to thirty thousand feet or so. As one raises the horizon point to a level where the density of the atmosphere is less the refraction correction, α, decreases--in fact it decreases roughly as the density decreases, a relation which will be used later. The complete expression, then, for the optical range, where the horizon point is at an elevation of h_h above sea level, is:

$$R \cong \sqrt{2(\rho + h_h)(h_m - h_h) + (h_m - h_h)^2 + (\rho + h_h)\alpha}$$

$$\cong \sqrt{2\rho(h_m - h_h) + (h_m - h_h)^2 + \rho\alpha} \qquad (8)$$

where $\rho + h_h$ is the new effective radius of the earth. Neglecting h_h relative to ρ results in an error in range of less than half of one per cent. The h_m is still defined as the altitude of the missile, M, above sea level. The angle, α, is now a function of h_h, and is given in Table 7 below. It is determined by extrapolating to zero angular altitude the refraction corrections found on the back of any recent issue of "The American Air Almanac" (Table A). Recall that this equation is derived on the assumption that the altitude h_m is large, so Equation (8) will be called the <u>high-altitude approximation</u>.

The above treatment must be modified when applied to a ray to or from an elevation which is as low as the altitudes attainable by aircraft. Now the refraction of the ray is still occurring at its upper end point, since

Table 7

Altitude (ft MSL)	Refraction Angle (min. of arc)	Density Ratio (ρ_h/ρ_o)
0	36	1.000
10,000	22	.739
20,000	17	.534
30,000	12	.376
40,000	7.5	.247

the aircraft is still within the relatively dense part of the atmosphere. It has been shown by actual experiments as well as by a theoretical treatment that the range from an aircraft to the sea-level horizon can be approximated very closely by the formula:[17]

$$R \cong 1.15 \sqrt{h'_a} = 1.09 \sqrt{2\rho h_a} \text{ n mi} \qquad (9)$$

where h'_a and h_a are the altitude of the aircraft in feet and in nautical miles respectively. (The mean radius of the earth, ρ, is about 3430 n mi.)

As shown in Eq. (6), the geometric range (neglecting refraction) is

$$R_g \cong \sqrt{2\rho h_a} \qquad (6')$$

where now the second term under the radical can be neglected because h_a is so much smaller than the earth's radius. It is obvious that the factor in front of the radical in Eq. (9) will decrease as the refraction effect decreases, and will approach unity in the second form of Eq. (9). In fact, this decrease will again be roughly proportional to the density at the

level of the effective horizon. Thus, Eq. (9) may be written in a more general form, involving the altitude of the horizon point, h_h, as:

$$R \cong \left(1 + .09\ \rho_h/\rho_o\right)\sqrt{2\rho(h_a - h_h)} \qquad (10)$$

where the density ratio, ρ_h/ρ_o, is the ratio of air density at the elevation of the horizon point, h_h, to the air density at sea level (see Table 7).

Equation (10) refers to the case where the aircraft is actually in the atmosphere at an altitude of 80,000 ft or less; it will be called the low-altitude approximation.

In drawing Fig. 9, using both the low-altitude and high-altitude approximations, the results show that both agree very closely at about 100,000 ft. It also turns out, as mentioned earlier, that the error which would be introduced if refraction were neglected entirely would be less than 10 per cent in range.

The discussion so far has been entirely general, in that only ranges between target and detector were discussed. Actually, in the case of the ICBM detection a more significant range may be that between missile launching site and detector, the missile moving toward the detector (assumed to be at the border of enemy territory) as it starts on its elliptical trajectory. The geometry of the missile path is shown in Fig. 11 (prepared by Hans Lieske, RAND Missiles Division). It is indicated in this figure that at burnout a 5500 n mi missile may be seen some 1400 n mi from the launching site by a detector at sea level, (X_{obs}), or 1600 n mi by a detector at 40,000 ft (see Fig. 9). This is 400 miles further than the range to the missile, the difference being due to the missile's horizontal motion up to burnout.

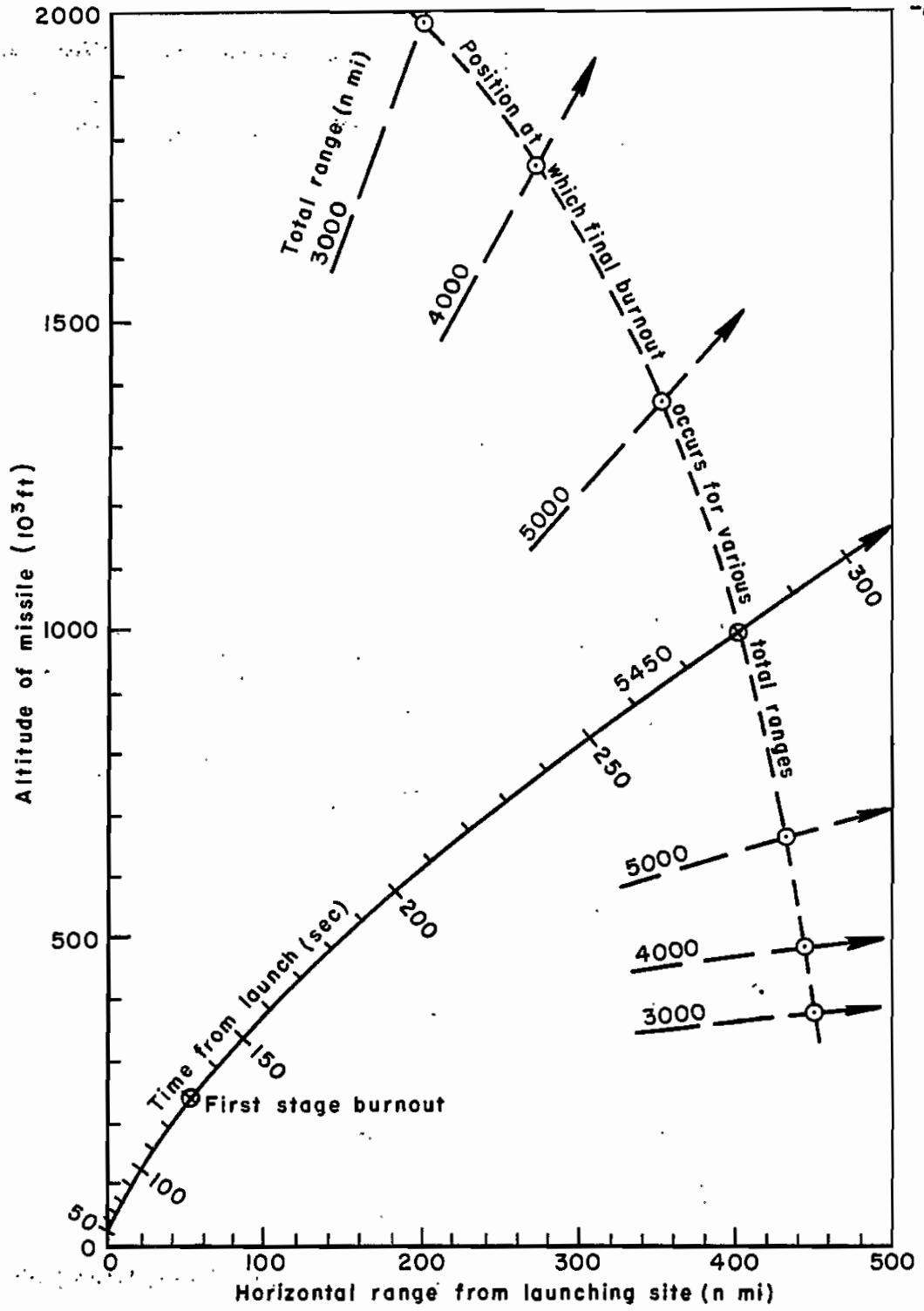

1572-11

Fig. 11 — The motion of a 5500 n mi ballistic missile during its take-off and early flight

Solid line represents maximum range trajectory; dashed lines indicate where final burnout would occur for same missile fired on shorter range trajectory.

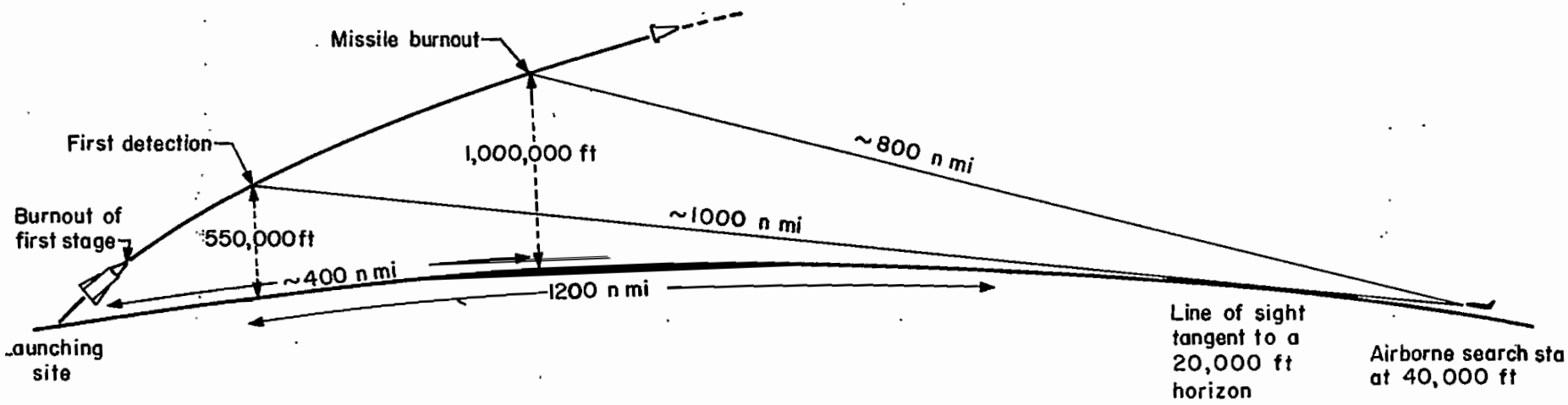

Fig. 12– Drawing (to scale) showing relative positions of ICBM take-off path and detector aircraft

To present more clearly the complete picture of both missile and detecting aircraft, Fig. 12 shows, to scale, the relative positions of the missile trajectory and the line of sight, assuming a 1200 n mi separation between launching site and aircraft. In the case shown, the missile is traveling on a great-circle course which would take it directly over the aircraft, though this is not a requirement for detection.

C. LIMITING SENSITIVITY OF AN INFRARED SEARCH SYSTEM

Consider an infrared search set in an aircraft flying at altitudes of the order of 40,000 ft (see Fig. 12). The extent of azimuthal search could be such that coverage of all anticipated launching sites could be accomplished with a small number of such "picket airplanes;" 60° is chosen as a reasonable design value. A search field slightly less than 10° in elevation is required to include the range of elevation angles covered by the ICBM between the time when it just clears the horizon and the point at which final rocket motor burnout occurs (about 10^6 ft), assuming an aircraft-to-launching site range of about 1,200 miles.

As seen from Fig. 12, an ICBM from a launching site 1200 n mi distant can be first observed from a 40,000 ft observation platform when it is at an altitude slightly over 550,000 ft (assuming an effective horizon at 20,000 ft). The missile at this point has been traveling for about 195 sec, and burnout will occur at 280 sec. The rate of change of the average line-of-sight of the ICBM is thus $\frac{10^\circ}{85 \text{ sec}} = 0.12^\circ/\text{sec}$. If the infrared scanning system is designed so that two looks are desired at the target at any position of the instantaneous field of view, (this will permit the use of some alarm system with a low false-alarm rate) then the angular motion of the line of sight during the time required to scan the whole field of

view, t_f, should be $\frac{\theta_i}{2}$, where θ_i is the angular diameter of the instantaneous field of view. Thus,

$$0.12^\circ/\text{sec} \times t_f = \frac{\theta_i}{2} \tag{11}$$

The dwell time of the target image on the detector, t_D, is given by the relationship:

$$t_D = \frac{\Omega_i}{\Omega_{total}} \times t_f \tag{12}$$

where Ω_i is the solid angle of the instantaneous field of view and Ω_{total} is the entire field of view to be scanned ($10^\circ \times 60^\circ$).

Taking the dwell time as the same order of magnitude as the detector time constant (2,000 μ secs for the cooled lead sulfide cell, which would be used to give maximum sensitivity to the high-temperature rocket flame source) and substituting in Eq. (12):

$$600^{\circ 2} \times 2 \times 10^{-3} \text{ secs} = t_f \times \pi \frac{\theta_i^2}{4} \tag{13}$$

Solving simultaneous Eqs. (11) and (13) for θ_i, the instantaneous field of view, and t_f, the scanning time, results in:

$$\theta_i = 0.7^\circ$$

$$t_f = 3 \text{ secs}$$

The aperture of this search system might be as large as 20 inches in diameter. For this aperture size and the instantaneous field of view of 0.7° the optical sine condition would determine the minimum detector element

size. (Detection using a single cell, rather than an array with duplication of electronic circuitry, etc., is assumed.) Assuming the PbS cell to be immersed in a medium of refractive index 1.5 results in a minimum cell size of 2 mm by 2 mm.

The amplifier bandwidth is chosen to contain the greater part of the pulsed waveform signal, which for a point target image would be $f_{max} = \frac{1}{t_D}$, $f_{min} = \frac{1}{t_f}$. For the system parameters given above reasonable values are $f_{max} = 500$ cps, $f_{min} = 1$ cps..

The over-all search system threshold sensitivity can be expressed by a relationship similar to Eq. (2), slightly altered to take into account the different scanning method. Thus:

$$P_T = G \times \frac{1}{\left(1 - e^{-t_d/\tau_D}\right)} \times S \times \frac{\sqrt{A_D}}{A_{eff.}} \times \sqrt{\log_e \frac{f_{max}}{f_{min}}} \qquad (2')$$

with P_T in effective watts/cm^2 at the aperture. (For explanation of symbols, see the discussion of Eq. (2).)

Employing a cooled (-78°C) lead sulfide cell in a detection system with the following characteristics

S at 2.5μ = 4.4×10^{-11} watts

τ_D = 2000 μ secs

effective aperture = 800 cm^2 (20 inch diameter collector, taking into account losses and occlusion)

G = 5

f_{max} = 500 cps

f_{min} = 1 cps

the resulting system threshold sensitivity, from Eq. (2') is

$$P_T = 2 \times 10^{-13} \text{ effective watts/cm}^2$$

D. MAXIMUM DETECTION RANGES DURING TAKE-OFF

It is now possible to determine the maximum detection ranges of the system for detection of the take-off phase of the ICBM, using the range equation, Eq. (1), the source radiant intensity given in Table 6, and values of the cell spectral efficiency shown in Fig. 3.

A factor must now be considered which was not included in the calculations of the previous chapter, the attenuation of the infrared radiation due to atmospheric absorption and scattering. A ray which leaves the missile (outside the atmosphere), passes tangent to the top of a cloud or haze layer at 20,000 feet, and then continues on to a detection station at 40,000 feet, penetrates through almost half of the total atmosphere twice. The air above 20,000 feet has less water vapor per gram of air than at sea level (it has a lower mixing ratio and dew point), but the ray described above must still pass through about 20 cm of precipitable water vapor on the average. Because of the decreased pressure, this amount of water vapor absorbs somewhat less effectively than it would at sea level, and we can consider the equivalent of about 15 cm of effective precipitable water vapor under standard pressure conditions as being in the path. This amount of water vapor results in about 50 per cent transmission in the infrared between 1.1 and 2.7 μ (the PbS region).[18]

The effect of atmospheric scattering at about 2μ is not nearly so great as in the visible, but the transmission factor of the same path due to scattering is around 70 per cent, bringing the total transmittance of

the air path tangent at 20,000 feet down to about 35 per cent. It should be remembered that when the missile is seen a degree or two above the apparent horizon the transmittance of the path will be nearly unity, due to the decreased optical depth of the path.

The results of combining these factors are shown in Table 8. The emission was calculated on the assumption that the missile was being viewed from the "forward quarter" (see Table 6). It is clear that when the missile is at a low altitude, some of the ranges given are far greater than can actually be achieved in view of the geometry of the situation. The significance of these large ranges is merely that the signal at operationally useable ranges is far above the threshold for detection.

In Fig. 13 the situation is summarized graphically. During the early stages of the takeoff there is more than enough infrared emission, but the earth gets in the way. Near burnout, when the missile is at about one million feet, the maximum infrared detection range and the geometry of the situation give comparable answers. After burnout there is not nearly enough infrared signal to give detection at any useful range. Recall that, depending on the trajectory of the missile and the location of the detection site, the launching site can be from 200 to 400 miles further away, due to the horizontal travel of the missile up to burnout (see Fig. 11).

The figures of Table 8 lead one to speculate on the increased warning time and perhaps more accurate trajectory prediction that might be possible by getting around this geometrical limitation with a very-high-altitude search station--perhaps with a satellite-borne infrared search set. This is the subject of a separate study at RAND.

Table 8

CALCULATION OF MAXIMUM INFRARED DETECTION RANGE OF AN ICBM DURING TAKE-OFF WHEN SEEN NEAR THE HORIZON FROM THE FORWARD QUARTER ASPECT

Altitude of Missile (1000 ft)	Time from Take-off (sec)	Flame Emission		Skin Emission		Infrared Detection Range* (n mi)
		Effective Temp. (°K)	Total Emission (kw)	Effective Temp. (°K)	Total Emission (kw)	
50	66	2400	11,000	375	60	9,000
200	120	2300	5,700	575	310	6,600
400	165	2200	920	520	48	2,700
800	245	2100	100	435	22	890
1,000	280	2100	100	400	16	890
1,500	365	--	0	370	10	34**

*Min. detectable flux at detection system: $P_T = 2 \times 10^{-13}$ effective watts/cm^2. Detector uses cooled PbS cell. Altitude of detector about 40,000 ft, effective horizon at about 20,000 ft. Transmittance of path is .35, except as noted.

**Assumed to be above the horizon, so atmosphere transmittance here is unity. The emission is characteristic of the lower surface in the daytime (Table 9).

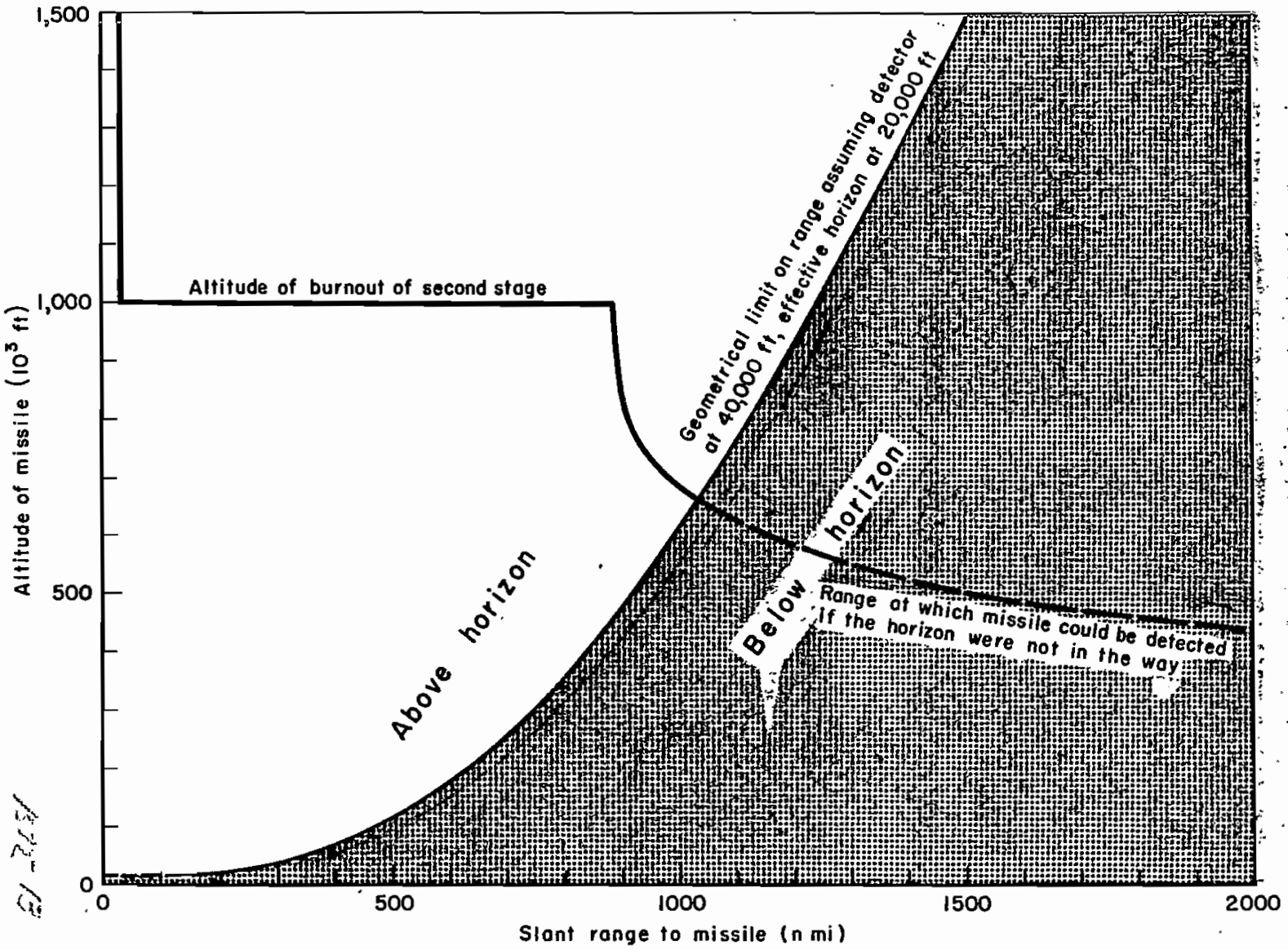

RM-1572
10-21-55
-52-

Fig. 13—The ranges of which on ICBM can be seen by on airborne infrared detector during its takeoff

IV. DETECTION OF AN ICBM DURING ITS MIDCOURSE FLIGHT

A. ICBM EMISSION DURING MIDCOURSE FLIGHT

Consider the temperature history of a long-range missile during its flight through and outside of the sensible atmosphere. The skin temperature during take-off climbs to nearly 600°K (see Table 5), reaching its maximum when the missile is at an altitude of about 200,000 ft. Thereafter it cools by radiative loss, and at burnout (near 1,000,000 ft) the temperature is between 450°K and 400°K and still falling toward a condition of radiative equilibrium.

The missile may be expected to have an emissivity of approximately 0.8 in the infrared (representative of oxidized steel or iron, aluminum oxide or a ceramic surface) and approximately 0.5 in the visible part of the spectrum. If the missile skin were made of polished steel, the diffuse emissivity and absorptivity would be less by a factor of two or three at all wavelengths. Since all wavelengths would be affected, the difference in radiative equilibrium temperatures would not be greatly affected by polishing the surface.

The skin temperature, then, assuming radiative equilibrium outside the atmosphere, will be approximately as shown in Table 9.

At these relatively low temperatures, the maximum detection range with equipment employing a photoconductor cell can only be a few tens of miles. For example, the extremely sensitive cooled lead sulfide detection system described in the previous section for detecting an ICBM during take-off can see the missile looking upward in the daytime at a maximum range of less than 50 miles. A lead telluride system similar to that described in Chapter II, even allowing for a doubling of the aperture size, would not do

Table 9

SKIN TEMPERATURE AND INFRARED EMISSION

OF AN ICBM IN MIDCOURSE FLIGHT

Time	Surface of Missile Relative to the Earth	Temperature for Radiative Equilibrium (°K)	Total Emission Normal to Axis (Area 20 m^2) (kw)
Day	Upper	390	21
Day	Lower	340	12
Night	Upper	<30	~ 0
Night	Lower	250	3.6

significantly better (maximum range $<$ 100 mi). Recall that the missile is at an altitude of about 200 miles at burnout, going up to apogees as great as 800 to 1000 miles.

Reflected sunlight will somewhat increase the infrared detection range if the detecting system uses no filters to discriminate against stars. However, for this daytime or near sunset observation, it would be better to employ detection equipment using photo-emissive devices with their superior time-constant and inherent short-wavelength sensitivity properties. A discussion will now be given of the maximum range performance of such equipment analogous to the discussions of detection ranges in Chapters II and III.

B. INTENSITY OF REFLECTED SUNLIGHT SIGNAL

The intensity of reflected sunlight as seen by airborne or ground detection equipment is a function of the relative angles between the axis

of the missile and the sun, θ_1, and the axis of the missile and the observer, θ_2, as well as being a function of the surface geometry of the missile. It will suffice for our order-of-magnitude calculation to assume that the missile body appears as a flat diffuse reflecting surface with a projected area of approximately 14 square meters. This area is characteristic of missile type 3 in Table 1, as seen from the forward quarter after burnout. The total radiant intensity of diffusely reflected sunlight off the missile surface is given by Lambert's law as:

$$E = \frac{i_o \times A \times \cos(\pi/2 - \theta_1) \cos(\pi/2 - \theta_2) \times \rho}{\pi} \text{ watts/steradian of reflected sunlight}$$

where

i_o = solar constant, 0.14 $\frac{\text{watts}}{\text{cm}^2}$

A = projected area of the missile, assumed = 14 m^2

ρ = diffuse reflectivity of missile surface, assumed $\sim$0.5

For an order-of-magnitude calculation, an aspect has been assumed such that the mean value of $\cos(\pi/2 - \theta_1) \cos(\pi/2 - \theta_2) = 0.4$. This gives

$$E = 1240 \text{ watts/steradian}$$

It is interesting to calculate the visual magnitude of such a body when observed at distances of the order of 1000 n mi. For light of the spectral characteristics of sunlight, 1 watt = 84 lumens. Thus, at this range, the intensity is equal to 3.05×10^{-12} $\frac{\text{lumens}}{\text{cm}^2}$. Now the visual magnitude, M, is related to the incident flux, I, by the following relationship[12]

$$\log_{10}\left(\frac{I_1}{I_2}\right) = 0.4\left(M_2 - M_1\right)$$

with the scale set at $M_2 = +1$ when $I_2 = 8.32 \times 10^{-11} \frac{\text{lumens}}{\text{cm}^2}$. Thus the ICBM will appear by reflected sunlight at missile-observer ranges of about 1000 n mi as an object of visual magnitude + 4.6.

Since the threshold of vision corresponds to a visual magnitude M = 6.8, it is clear that near twilight and for some time after sunset, depending on latitude and season, it will be possible for a not-too-distant visual observer to see the ICBM during a portion of its trajectory.

C. SENSITIVITY OF A PHOTOELECTRIC DETECTION SYSTEM

For the daytime application of an airborne photoelectric search system, even operating at high altitude and at small zenith angles, the limiting noise of the system will be photon shot noise due to the background sky brightness. In a detailed derivation of the sensitivity of their photon-noise limited "Hook" equipment for air-to-air search application, the Scripps Visibility Laboratory[19] has derived photoelectric detection ranges for the detection of the so-called "contrast signal" due to sky obscuration by the target aircraft. For the present application, the "Hook" work has been modified to calculate detection ranges of the ICBM using reflected sunlight.

The threshold sensitivity, P_T, in effective watts/cm^2 at the aperture of the photoelectric detection system, for the background-photon-noise-limited condition, can be shown to be:

$$P_T = 1.5 \times 10^{-13} \times G \sqrt{\frac{N\Omega\Delta f}{A_{eff} S}} \quad \frac{\text{effective watts}}{\text{cm}^2}$$

where,

G = minimum signal-to-noise level needed for reliable detection

A_{eff} = effective aperture area, with correction for optical losses, in cm^2

N = sky brightness, in foot-lamberts

Δf = amplifier bandwidth, in cps

Ω = instantaneous field of view of the scanning system, in steradians

S = photo-cathode sensitivity in amp/watt for sunlight

The "Hook" air-to-air search system described in Ref. (19) scans a $10^{\circ} \times 40^{\circ}$ sector of the sky in a total frame time of 2 secs. It utilizes 21 phototubes in scanning the image space of a 4-inch lens by means of punched diaphragms in a moving belt. Parameters for this system are:

$A_{eff} = 64\ cm^2$

$\Delta f = 3000$ cps

$\Omega = 2 \times 10^{-6}$ steradian

S, for the K1211 phototube employed is 0.01 amp/watt

For a high-altitude (40,000 ft) airborne search at moderate to small zenith angles, the sky brightness, N, is likely to be of the order of 100 foot-lamberts.[20] Hence, for this equipment, the threshold sensitivity, assuming a minimum signal to noise ratio, G, of 2 is:

$P_T = 3 \times 10^{-13}$ effective watts/cm^2 at the detection system aperture.

D. DETECTION RANGES

The range of detection for the photoelectric system can now be estimated using the range equation,

$$R_{max} = \sqrt{\frac{E\eta_D}{P_T}}$$

assuming negligible attenuation of this visible radiation at the very high altitude considered here.

The spectral efficiency of this photoelectric detector for radiation of the spectral quality of sunlight, η_D, is approximately 0.15.

Substituting E = 1240 watts/steradian

$$\text{and} \quad P_T = 3 \times 10^{-13} \text{ effective watts/cm}^2$$

results in maximum daylight detection ranges of the ICBM by this equipment of only about 135 n mi.

It might be worth while to consider a combination infrared-photoelectric detection system, with the infrared search set used to detect the ICBM from takeoff to soon after burnout and serving to position the photoelectric detector to this region of the sky so that it need only track the remainder of the mid-course trajectory. For this tracking application, with the rather small rotation rates of the line of sight involved, the requirements on bandwidth could be reduced so that bandwidths, Δf, of 50 to 100 cps might be considered. In this case one would get an improvement in daylight detection ranges of

$$\sqrt[4]{\frac{3000}{50}} \simeq 2.8$$

so that detection ranges of about 400 n mi might be achieved. These ranges appear rather inadequate for the generation of any further trajectory information beyond that which would be achieved by the initial infrared detection phase.

After sunset, the background photon noise drops to nearly the thermionic

shot noise level, so that improvements in the photoelectric detectivity of the order of 1000 are possible. Hence, if the ICBM is not eclipsed by the earth's shadow, detection ranges of many thousands of miles are possible. With the exception of arctic regions at particular seasons, this period of visibility must be rather short, being just before sunrise or after sunset.

It should also be pointed out that for any of the photoelectric detection systems discussed here some sort of discrimination against the many celestial objects of greater radiance in this visible region must be invented.

This section has only touched on some of the problems involved in the mid-course optical detection of ICBM's. While these problems do not appear to be insuperable, they are grave enough and their solution is of such limited applicability as to make this aspect much less promising than the use of infrared techniques during the take-off and re-entry phases. Specifically, it should be noted that the nighttime detection is apparently less than marginal, and a system which could operate only in the daytime or at twilight can hardly be relied upon.

V. FIELDS FOR FURTHER RESEARCH

It is evident that there is uncertainty in some of the estimates which have been made in the preceding chapters. This uncertainty may, of course, be due to the fact that we cannot guess exactly what the characteristics of the Russian ICBM will be, and in such a case we must base our judgment on the whole range of possibilities. In other cases, however, our limitations are simply due to a lack of basic knowledge of factors over which the Soviet designer has little or no control. These areas, which require further research, will be summarized briefly.

A. RE-ENTRY

1. Skin Temperatures

The problem of the heating of the skin of a hypersonic re-entry body is a basic consideration in the design of an ICBM system. For this reason, a considerable amount of effort is already being devoted to it. It is, perhaps, worth mentioning that, whereas the missile designers are most concerned with the maximum temperature to which the re-entry body will be exposed, which usually occurs at altitudes below 100,000 ft, infrared detection systems are most concerned with the heating which occurs higher up, as the re-entry body first encounters the denser atmosphere, together with knowledge of its emissivity.

2. Radiation from Air Excited by the Shock Wave

In some sense the problem of emission by air in hypersonic flow is closely related to that of skin heating, since under certain conditions at relatively low altitudes the skin may receive considerable heat from this radiation. However, the detection problem may be greatly influenced

by the shock wave emission while the re-entry body is still high in the atmosphere, at altitudes of several hundreds of thousands of feet. If there were strong emission from the excited air in the shock wave (or in the trail) of an ICBM, this would certainly increase the ease of early optical detection.

3. Optimization of the Infrared Search-Track Detection Process

As discussed in Chapter II, the use of an infrared or optical detection system for terminal guidance in an ICBM defense missile requires consideration of a large number of system design factors. There is much to be done in the optimization of such a seeker system, and the theory for the most efficient method for combining the information is inadequate. Scanning system techniques, bandwidth considerations, infrared detector properties, seeker angular accuracy, etc., are all areas requiring further attention.

B. TAKE-OFF

1. Rocket Emission

The chief source of radiation during the powered phase of an ICBM is certainly the rockets. However, the most crucial part of the take-off from the point of view of detection is the latter part of the powered flight, while the missile is above the horizon for a distant observing station. It is here that a great deal of uncertainty exists about the characteristics of a rocket flame. (See the discussion in Section III.A.) The description of the emission of a rocket in an almost perfect vacuum can be achieved by:

(a) Theoretical calculations of the thermal emission from the exhaust gases, a mixture of CO, CO_2, OH, H_2O, CH, and some metallic impurities, plus nitrogen compounds for certain fuels such as acid-aniline. This is a difficult calculation, and is complicated by uncertainties as to the

relative amounts of the various constituents, which depend on the fuel-oxygen mixture.

(b) Observations of rocket flames in a vacuum or in an inert atmosphere. This kind of observation could presumably be done in a laboratory, and would yield valuable information. No opportunity should be missed, of course, to make observations on an actual rocket at comparable altitudes.

2. Interaction of a Missile with the Upper Atmosphere

This is an area which is difficult to define, since so little is known about it. There are a few phenomena which might conceivably be capitalized upon in order to achieve a better ICBM detection capability, but they can only be suggested in the most general terms.

(a) Excitation and ionization of the gaseous envelope. As the rocket passes through the ionosphere it will have enough speed to excite and ionize the air. Though the density is exceedingly low, it is possible that such a large body will create a glowing trail of luminous gas, like an auroral streamer (such streamers being observed at altitudes of up to about 500 mi).

(b) Creation of magneto-hydrodynamic waves in the ionosphere. A perturbation in a plasma imbedded in a magnetic field is propagated as a quasi-electromagnetic wave at velocities which are considerably greater than the "speed of sound" (though sound has no physical meaning in the ionosphere in the conventional sense). The magneto-hydrodynamic waves traveling out from an ascending ICBM might be detected at considerable ranges. This question is currently being explored by Zwicky at C.I.T., under the sponsorship of the Air Force Office of Scientific Research.

REFERENCES

1. Kellogg, W. W., and S. M. Greenfield, Infrared Radiation for the Detection of Airborne Targets, The RAND Corporation, Research Memorandum RM-784, April 1, 1952 (Confidential).

2. Tieman, C. R., Infrared Reception and Its Application to Missile Guidance, Aeronautical Research Center, University of Michigan, Project Wizard Report UMM-27, 1948 (Secret).

3. Gazley, C., Heat Transfer Aspects of the Atmospheric Re-Entry of Long-Range Ballistic Missiles, The RAND Corporation, Research Report R-273, August, 1954. (Secret).

4. Graham, W. B., A Preliminary Discussion of Intercontinental Ballistic Missile Defense, The RAND Corporation, Research Memorandum RM-1495, May 16, 1955 (Secret).

5. Kirby, R., Consolidated Vultee Aircraft Corp., personal communication, 1955.

6. Meyerott, R., The Absorption Coefficients of Air at Temperatures Below 18,000°K, The RAND Corporation, Research Memorandum RM-1554, August 24, 1955.

7. Jones, R. Clark, "Performance of Detectors for Visible and Infrared Radiation," in Advances in Electronics, edited by L. Marton, Vol. 5, Academic Press, New York, 1953.

8. Blumenthal, I.S., A Potential Interceptor for Defense Against the Intercontinental Ballistic Missile--The One-Eyed Goalie (title Confidential, The RAND Corporation, Research Memorandum RM-1389, December 15, 1954 (Secret).

9. Blumenthal, I.S., Threshold Guidance for the One-Eyed Goalie--A Potential Interceptor for Defense Against the ICBM, The RAND Corporation, Research Memorandum RM-1514, July 8, 1955 (Secret).

10. Schiff, L. I., Scanning Systems and Color Filters, Project Metcalf, Brown University, Final Report, Vol. 2, October, 1952 (Secret).

11. Hughes Aircraft Company, Progress reports in connection with USAF Missile Project MX-904 (GAR-1B, Falcon), Contract AF33(600)24231, 1954.

12. Larmore, L., Infrared Radiation from Celestial Bodies, The RAND Corporation, Research Memorandum RM-793-1, June 26, 1952 (Confidential).

13. Jones, S., The Two-Color Optical Chopper, Telecommunications Research Establishment (U.K.), Memorandum 676, 1952.

14. Bundy, F. P., R. H. Johnson, and H. M. Strong, Final Report on Optical Studies of Rocket Flame at Malta Test Station, General Electric Company, Project Hermes Report R50A0506, 1950.

15. Curcio, J. A., and J. A. Sanderson, Further Investigations of the Radiation from Rocket Motor Flames, Naval Research Laboratory, Dept. of the Navy, Report N-3327, 1948 (Confidential).

16. Wyman, F. E., Relative Radiation Density and Temperature Distribution of Rocket Flames, Naval Research Laboratory, Dept. of the Navy, Report 3823, 1951.

17. Russell, H. N., R. S. Dugan, and J. Q. Steward, Astronomy, rev. ed., Vol. I, The Solar System, Ginn and Co., 1945, p. 105.

18. Elder, T., and J. Strong, "The Infrared Transmission of Atmospheric Windows," Jour. Franklin Inst., Vol. 255, No. 3, pp. 189-208, 1953.

19. University of California Scripps Institution of Oceanography, Visibility Laboratory, Status Report on Air-to-Air Target Acquisition Equipment for Day Fighter Aircraft, Report NS 714-100, February, 1955 (Confidential).

20. Packer, D. M., and C. Lock, Brightness and Polarization of the Daylight Sky at Altitudes of 18,000 and 38,000 Feet Above Sea Level, Naval Research Laboratory, Dept. of the Navy, Report 3713, Washington, 1950.